Systematic analysis of the R2R3-MYB family of transcription factors in *Camellia sinensis*: evidence for species-specific catechin biosynthesis regulation

Jingyi Li[a,1], Shaoqun Liu[a,1], Peifen Chen[a], Jiarong Cai[a], Song Tang[a], Wei Yang[a], Fanrong Cao[a], Peng Zheng[a,*] and Binmei Sun[a,*]

a. Key Laboratory of Biology and Germplasm Improvement of Horticultural Crops in South China, Ministry of Agriculture, College of Horticulture, South China Agricultural University, Guangzhou 510642, People's Republic of China

[*]Corresponding author (P. Zheng and B. Sun) at: Room 603, College of Horticulture, South China Agricultural University, Guangzhou 510642, People's Republic of China.

E-mail address: zhengp@scau.edu.cn (P. Zheng), binmei@scau.edu.cn (B. Sun)

1 These authors contributed equally to this work.

Abstract

Tea from *Camellia sinensis* is one of the most popular beverages worldwide, lauded for its charming flavors and health-promoting properties. *C. sinensis* produces an abundance of specialized metabolites, which makes it an excellent model for digging into the genetic regulation of plant-specific metabolite biosynthesis. The most abundant health-promoting metabolites in tea are galloylated catechins, and the most bioactive of the galloylated catechins, epigallocatechin gallate (EGCG), is exclusively found in *C. sinensis*. The R2R3-MYB transcription factor family regulates metabolism of phenylpropanoids, the precursors to catechins, in various plant lineages. However, the transcriptional regulation of galloylated catechin biosynthesis remains elusive. Species-expanded or specific MYB transcription factors may regulate species-specific metabolite biosynthesis. This study mined the R2R3-MYB transcription factors associated with galloylated catechin biosynthesis in *C. sinensis*. A total of 118 R2R3-MYB proteins, classified into 38 subgroups, were identified. R2R3-MYB subgroups specific to or expanded in *C. sinensis* were hypothesized to be essential to evolutionary diversification of tea-specific metabolites. Notably, nine of these *R2R3-MYB* genes were expressed preferentially in apical buds and young leaves, exactly where galloylated catechins accumulate. Three putative *R2R3-MYB* genes displayed strong correlation with key galloylated catechin biosynthesis genes, suggesting a role in regulating biosynthesis of epicatechin gallate (ECG) and EGCG. Overall, this study paves the way to reveal the transcriptional regulation of galloylated catechins in *C. sinensis*.

Keywords: *Camellia sinensis*, galloylated catechins, R2R3-MYB, transcriptional regulation, catechin biosynthesis

Introduction

Tea from *Camellia sinensis*, along with coffee and cocoa, is one of the world's three major non-alcoholic beverages. Worldwide, approximately two billion cups of tea are consumed daily (Drew et al., 2019; Yamashita et al., 2020). Tea production has amplified at an average annual rate of 3.35%

in the last five years; by 2019, worldwide tea production reached 6.49 million tons on 5.07 million hectares (Food and Agriculture Organization of the United Nations statistics, https://www.fao.org/faostat/). Tea was used first as a food in ancient China, then it served as a medicine to prevent and cure common diseases before developing into a popular beverage (Abbas et al., 2017; Mondal et al., 2004). Nowadays, tea exhibits great commercial potential and has become a vital industry due to its health promoting properties and attractive distinct flavors (Chen et al., 2009).

The tea plant (*C. sinensis*) is rich in characteristic metabolites, such as polyphenols, amino acids, caffeine, and terpenes, that significantly contribute to its pleasant flavors and industrial and medical value (Wei et al., 2018). Catechins are the principal health-promoting bioactive compounds of tea. Catechins constitute 12 to 24% of the dry weight of young leaves, and account for more than 70% of the total polyphenols (Yang et al., 2012). Catechins in tea consist of a mixture of catechin (C), epicatechin (EC), gallatechin (GC), epigallocatechin (EGC), catechin gallate (CG), epicatechin gallate (ECG), gallatechin gallate (GCG) and epigallocatechin gallate (EGCG) (Asakawa et al., 2013). Among them, galloylated catechins ECG and EGCG are abundant in tea plants and account for more than 80% of total catechins (Kim et al., 2004; Liu et al., 2012). EGCG, exclusively present in *C. sinensis*, is the major bioactive component conferring the many health benefits of tea - it is anti-carcinogenic (Ahmad et al., 2000), anti-oxidative (Heim et al., 2002), anti-bacterial and anti-inflammatory (Taguri et al., 2004) and it prevents cardiovascular and cerebrovascular diseases (Yu et al., 2020). In addition, EGCG is widely used in food production on account of its strong antioxidative capacity(Nikoo et al., 2018).

To date, based on biochemical, physiological and genetic research, the biosynthesis pathway of catechins has become clear (Wei et al., 2018; Yang et al., 2012; Yu et al., 2021). Catechins are derived from the phenylpropanoid pathway and principally accumulate in apical shoots and young leaves. Galloylated catechin content is mainly regulated at the transcriptional level by catechin biosynthesis genes *dihydroflavonol reductase* (*DFR*), *anthocyanidin reductase* (*ANR*), *leucoanthocyanidin reductase* (*LAR*) and *serine carboxypeptidase-like acyltransferases* (*SCPLs)* (Ashihara et al., 2010; Eungwanichayapant et al., 2009; Punyasiri et al., 2004; Singh et al., 2008;

Wei et al., 2018). However, few studies have focused on the network(s) that regulate catechin biosynthesis, especially galloylated catechins.

R2R3-MYB transcription factors (TFs) comprise the largest family of TFs in advanced plants (Ambawat et al., 2013). In addition to possessing two imperfect MYB repeats (R2 and R3), the R2R3-MYB TFs maintain a highly conserved N-terminal MYB DNA-binding domain and an activated or repressed C-terminal domain (Dubos et al., 2010; Jiang et al., 2004; Jin and Martin, 1999; Kranz et al., 1998; Lipsick, 1996; Martin et al., 1997). The R2R3-MYB family is widely involved in plant growth and development, primary and secondary metabolism, hormone signal transduction, cellular proliferation and apoptosis, as well as disease and abiotic stress response (Li et al., 2017; Martin et al., 1997). Notably, the R2R3-MYB family plays an important role in positively or negatively regulating the biosynthesis of specialized metabolites, such as flavonoids (Hichri et al., 2011; Mehrtens et al., 2005), anthocyanin (Li et al., 2020; Li et al., 2017; Yu et al., 2020) and lignin (Bedon et al., 2007; Goicoechea et al., 2005).

Studies have found that new R2R3-MYB TFs emerged through species-specific duplication events (Soler et al., 2015). Species-specific evolved or expanded R2R3-MYB membership seems to confer functional diversification to organisms (Zhang et al., 2000). For example, the ancestral R2R3-MYB anthocyanin master regulator expanded into several homologous clusters within the grape (*Vitis* spp.) and maize (*Zea mays*) genomes, and differential expression of duplicated genes resulted in control of anthocyanin biosynthesis in different tissues (Jiu et al., 2021; Zhang et al., 2000). Some species-specific and expanded *R2R3-MYB* TFs govern specialized metabolite biosynthesis within lineages (Zhu et al., 2019). In *Capsicum*, five Solanaceae-specific MYB TF tandem genes duplicated in the *Cap1/Pun3* locus. *Capsicum* species have evolved placenta-specific expression of MYB31, which directly activates expression of capsaicinoid biosynthetic genes and results in production of genus-specialized metabolites. In *C. sinensis*, only a few R2R3-MYB transcription factors have a demonstrated role in regulation of phenylpropanoid biosynthesis. Specifically, *CsAN1*, *CsMYB6A* and *CsMYB75* regulate anthocyanin pigments in *C. sinensis* leaf (He et al., 2018; B. Sun et al., 2016; Wei et al., 2019). However, the *C. sinensis* specific and expanded R2R3-MYB TFs that are potential candidate regulators of galloylated catechins

biosynthesis have still not been identified.

In this study, through performing a genome-wide analysis of the R2R3-MYB superfamily in *C. sinensis*, we compared the phylogenetic relationships between *C. sinensis* and other plant lineages. The gene structure, conserved motifs and transcript patterns were analyzed. Because of the importance of galloylated catechins in *C. sinensis*, we focused on the discovery of *R2R3-MYB* genes potentially involved in the regulation of biosynthesis of ECG and EGCG, especially EGCG which is unique to *C. sinensis*.

Materials and Methods

Plant materials

The 'Lingtoudancong' variety of *C. sinensis* was grown at South Agricultural University in Guangzhou, China. Apical buds, first leaves, second leaves, mature leaves, old leaves, stems and roots of 'Lingtoudancong' were sampled in spring of 2021. The samples of different tissues were immediately frozen in liquid nitrogen and stored at -80°C.

Phylogenetic analysis

C. sinensis MYB protein sequences were retrieved from the Tea Plant Information Archive database (http://tpia.teaplant.org/). In total, 222 MYBs and MYB-related genes were predicted in the 'Shuchazao' genome, but only 118 of these had two consecutive and conserved repeats of the MYB domain. The R2R3-MYB protein sequences of *Arabidopsis thaliana* were obtained from the Arabidopsis Information Resource Archive database (https://www.arabidopsis.org/). The number of R2R3-MYB gene models identified by our methodology in the genome of *A. thaliana* (126) was the same as described in the literature (Dubos et al., 2010). The homologous genes of kiwifruit, coffee, cacao and grape were retrieved from the Plant Transcription Factor Database (http://planttfdb.gao-lab.org/) by performing a reverse BLAST search. All the R2R3-MYB sequences were aligned using ClustalX, and a neighbor-joining phylogenetic tree was constructed with 1,000 bootstrap replicates utilizing MEGAX (Kumar et al., 2016). A pairwise deletion method was chosen to dispose of the

positions containing gaps or missing data in the sequences, and the delay divergent cutoff value was set to 30.

Conserved motif analysis of R2R3-MYB

Functional motifs and conserved domains were identified with The MEME Suite tool (https://meme-suite.org/meme/) using the following parameters: site distribution, zero-or-one-site-per-sequence (ZOOPS) model; maximum number of motifs: 20; minimum motif width: 6; maximum motif width: 50; minimum number of sites per motif: 2; and maximum number of sites per motif: 118 (Bailey et al., 2009; Chen et al., 2021). The sequence logos of R2 and R3 repeats of the R2R3-MYB proteins were based on multiple sequence alignments and were visualized with WebLogo Version 2.8.2 (http://weblogo.berkeley.edu/logo.cgi). All obtained motifs were constructed and visualized using the Gene Structure View (Advanced) of the TBtools software (Chen et al., 2020).

RNA-seq expression analysis

The RNA-seq data were downloaded from TPIA for transcript abundance analyses. The expression levels of the candidate *R2R3-MYB* TFs and catechin biosynthesis genes from different tissues of *C. sinensis* were used to generate a heatmap with TBtools software using the normalized method.

RNA extraction and quantitative real-time PCR (qRT-PCR)

Total RNA of different tissues of 'Lingtoudancong' was extracted utilizing a Magen HiPure Plant RNA Mini kit B (R4151, Magen, China) according the manufacturer's instructions. First-strand cDNA was synthesized using a HiScript III RT 1st Strand cDNA Synthesis kit (R323-01, Vazyme, China) in a reaction volume of 20 μL. qRT-PCR was performed in a Bio-Rad CFX384 Touch™ system. Each 10 μL reaction mixture was comprised of 4.4 μL qPCR SYBR Green Master Mix (Yeasen, China), 4.4 μL double distilled water, 0.2 μL of each primer (10 μmol/μL) and 1 μL of cDNA template. The reaction program was as follows: 95 °C for 5 min; then 39 cycles at 95 °C for 5 s and 60 °C for 30 s. A melting-curve analysis was carried out at 95 °C for 5 s, which was followed by a temperature increase from 60 °C to 95 °C. *Actin* (*TEA019484.1)* was used as the housekeeping

gene. The relative expression of each gene was calculated with the $2^{-\Delta\Delta Ct}$ method (Livak and Schmittgen, 2001). The qRT-PCR primers were designed with the qPrimerDB-qPCR Primer Database (https://biodb.swu.edu.cn/qprimerdb/). Sequences of the primers are listed in Supplementary Table S2. Values were the means ± SDs of 3 replicates.

Quantification of catechin contents

Reference standards of catechin (C), epicatechin (EC), epigallocatechin (EGC), epicatechin gallate (ECG), and epigallocatechin gallate (EGCG) were purchased from Shanghai Yuanye Bio-Technology Co., Ltd. (Shanghai, China). Apical buds, first leaves, second leaves, mature leaves, old leaves, stems and roots of 'Lingtoudancong' were ground into fine powders and freeze-dried. Approximately 0.2 g of each sample powder was extracted with 8 mL of 70% methyl alcohol (diluted with ultrapure water). After ultrasonic extraction for 30 min, the supernatant was collected by centrifugation. 1 mL of the liquid supernatant was filtered through a 0.22 μm Millipore membrane. The extracts were injected into an XSelect HSS C18 SB column (4.6 × 250 mm, 5 μm, Waters Technologies, USA). The catechin monomers were separated using 0.1% aqueous formic acid (A) and 100% acetonitrile (B) as mobile phases on a Waters Alliance Series HPLC system (Waters Technologies, USA). Detection was performed at 280 nm. Data were presented as the mean ± SD (n = 3).

Correlation analysis of gene expression and metabolite accumulation

The correlation analysis among transcription factors, catechin biosynthesis genes and catechin monomer contents was performed via Pearson's correlation coefficients. The R software was adopted to visualize the relationship directly. A correlation coefficient of >0.5 was considered to be a positively associated pair, and R<-0.5 was thought of as a negative correlation. In the diagram, blue represents a positive correlation, and red represents a negative correlation.

Results

Comparative phylogenetic analysis of the R2R3-MYB families in *C. sinensis* and *A. thaliana*

A total of 118 *R2R3-MYB* genes were identified in the *C. sinensis* genome after manual curation and exclusion of alternative transcripts. All identified *R2R3-MYB* genes from *C. sinensis* (118) were aligned with those of *A. thaliana* (126), and their evolutionary history was inferred by constructing a neighbor-joining phylogenetic tree (Fig.1). The 118 *R2R3-MYB* genes of *C. sinensis* were named in light of the systematic naming rules of *A. thaliana*, except for *CsMYB1*, *CsMYB4a* and *CsAN1*, which had been functionally characterized previously (Li et al., 2017; Sun et al., 2016a; Yang et al., 2012) (Supplementary Table S1). In addition, as it is believed that genes which clustered together were considered to be in the same subgroup, and *A. thaliana* is, by far, the species for which the *R2R3-MYB* genes have been most extensively investigated, the 38 subgroups were classified by taking into account the topology of the tree and the bootstrap values (Fig. 1) and were named according to the classification of *A. thaliana* (Dubos et al., 2010). For new subgroups not previously proposed in *A. thaliana*, the subgroup was named after the known functionally characterized *A. thaliana* member.

The majority of subgroups contained members from both species. However, S12 was an *Arabidopsis*-specific subgroup, containing only *R2R3-MYB* members from *A. thaliana*. The members of subgroup S12, *AtMYB28*, *AtMYB29*, *AtMYB76*, *AtMYB34* and *AtMYB5*1 regulate glucosinolate biosynthesis, a metabolite exclusive to the *Brassicaceae* family (Gigolashvili et al., 2007; Matus et al., 2008). In contrast, three subgroups contained *R2R3-MYB* TFs that were present only in *C. sinensis* without any homologues in *A. thaliana*. Therefore, their names we designated as Tea Preferential Subgroup A (TPSA), Tea Preferential Subgroup B (TPSB) and Tea Preferential Subgroup C (TPSC). Remarkably, SMYB5 and S5 subgroups were comprised of more tea plant *R2R3-MYB* members than *A. thaliana* members. For example, subgroup S5 had three *C. sinensis* members (*CsMYB31*, *CsMYB32* and *CsMYB34*), while *A. thaliana* contributed only one member, *AtMYB123/TT2.* Similarly, the SMYB5 subgroup had four members from *C. sinensis* (*CsMYB37*, *CsMYB39*, *CsMYB42* and *CsMYB43*), but just one member (*AtMYB5*) from *A. thaliana.* In *Arabidopsis*, the members of SMYB5 and S5 subgroups are involved in the phenylpropanoid pathway. *AtMYB123* controls the biosynthesis of proanthocyanidins (PAs) in the seed coat and *AtMYB5* was partially redundant with *AtMYB123* (Gonzalez et al., 2009). The expansion of SMYB5

and S5 subgroups in *C. sinensis* suggests that diversified regulation of polyphenols emerged during the speciation of *C. sinensis*.

Overall, the phylogenetic analysis results highlighted five special subgroups TPSA, TPSB, TPSC, S5 and SMYB5, which expanded in or were exclusively present in *C. sinensis*. Among these subgroups, a total of 21 *R2R3-MYB* TFs (TPSA (6), TPSB (4), TPSC (4), S5 (3) and SMYB5 (4)) attracted our attention and were selected for further analysis as potential candidates involved metabolic processes specific to *C. sinensis*.

Functions inferred through phylogenetic analysis of the candidate subgroups in six plant species

To evaluate the 21 *R2R3-MYB* genes of the five tea-specific and tea-expanded subgroups TPSA, TPSB, TPSC, S5 and SMYB5, the homologous *R2R3-MYB* genes from kiwifruit, coffee, cacao, and grape were used to construct phylogenetic tree (Fig. 2). The number of *R2R3-MYB* TFs presented a trend of expansion in *C. sinensis* (21) similar to coffee (20), but greater than cocoa (11), kiwifruit (11) and grape (18). We surmised that the *C. sinensis* expanded *R2R3-MYB* function may have occurred through divergent evolution during speciation. For example, subgroup TPSA was expanded in tea (6) relative to coffee (3), cocoa (5), kiwifruit (5) and grape (1). In the TPSB subgroup, coffee (4), grape (4) and kiwifruit (3) had comparable numbers of members with *C. sinensis* (4), but only two homologous genes were found in cocoa. Subgroup TPSC contained homologous genes in all species except for kiwifruit. Remarkably, no isogenous genes of TPSA, TPSB or TPSC subgroups were present in *A. thaliana*, indicating that these *R2R3-MYB*s evolved only in tea plant and probably have novel functions.

To uncover the roles these *R2R3-MYB* genes serve, we searched for the functional characteristics of the selected *R2R3-MYB* genes from four close relative species. Only a few homologous genes (*GSVIVT01026868001*, *Achn38246* and *Achn172901* from the TPSA subgroup; *Achn143561*, *Achn322351* and *GSVIVT0103866001* from the TPSB subgroup; and *Thecc1EG029126t1*, *GSVIVT01016765001* and *GSVIVT01035467001* from TPSC subgroup) have been experimentally verified. In the TPSA subgroup, *GSVIVT01026868001* played an inhibitory role in flower

development (Velasco et al., 2007), while both *Achn38246* and *Achn172901* acted as transcriptional activators involved in cold stress response (Park et al., 2010; Savage et al., 2013). Homologous genes in the TPSB subgroup, *Achn143561*, *Achn322351* and *GSVIVT0103866001*, performed a similar role in regulating plant protection against UV stress (Schenke et al., 2014). The paralogous genes of subgroup TPSC (*Thecc1EG029126t1*, *GSVIVT01016765001* and *GSVIVT01035467001*) mainly regulated plant epidermal cell fate (Cheng et al., 2014; Savage et al., 2013). Above all, we ventured that the function of the TPSA, TPSB and TPSC subgroups in *C. sinensis* might associate with responses to biotic and abiotic stress along with influencing certain developmental processes.

Conserved motif analysis of *R2R3-MYB*s

The R2 and R3 MYB domains of the 118 *C. sinensis R2R3-MYB* TFs were analyzed (Fig.3). The R2 and R3 domains contain a set of characteristic amino acids, which include the highly conserved and evenly distributed tryptophan residues (Trp, W) known to be critical for sequence-specific binding of DNA (Cao et al., 2013; Stracke et al., 2001), demonstrating that the R2 and R3 MYB repeats of the MYB DNA-binding domain are highly conserved in *C. sinensis*, consistent with previous findings of the counterpart genes in other plant lineages (Du et al., 2012; Li et al., 2016; Wilkins et al., 2009). Most of the conserved residues were situated between the second and third conserved W residues in each MYB repeat, elucidating that the first area of them was less conserved than the other two.

Conserved amino acid motifs represent functional areas that are maintained during evolution. The conserved motifs within the 118 R2R3-MYB sequences were analyzed and aligned using MEME Suite (Bailey et al., 2009). A total of 20 conserved motifs were identified in the R2R3-MYB family (Fig. 4). Six of these, motifs 1 to 6, were present in all R2R3-MYB members except for CsMYB1a and thus were designated as “general motifs;” the rest of the motifs (motifs 7 to 20) were considered to be “specific motifs,” since they were present in only one or several R2R3-MYB members. For instance, motifs 16 and 9 were unique to CsMYB1a and CsMYB117a; meanwhile, motifs 15 and 19 were contained only in three genes. Overall, the members clustering to the same clade harbored similar motif patterns.

Expression patterns of the *R2R3-MYB* family

The expression patterns of 118 genes encoding *R2R3-MYB* TFs were analyzed in different tissues. No transcripts were detected for *CsMYB101* (*TEA028392.1*) and *CsMYB117b* (*TEA002233.1*), suggesting they are pseudogenes in *C. sinensis*. The genes were classified into seven expression clusters, based on their distinct transcript patterns in various tissues and organs (Fig. 5). The 21 genes in RNA-seq-based cluster 1 were expressed mainly in flowers; genes in cluster 2 (14) were predominantly expressed in fruits; genes in cluster 3 (29) were mainly expressed in tender roots; genes in cluster 4 (8) were expressed at comparable levels in both apical buds and tender roots; cluster 5 genes (18) were mainly present in apical shoots and young leaves; while cluster 6 genes (21) were mainly expressed in stems and finally, cluster 7 genes (5) were equally expressed in mature leaves, old leaves and stems. Normally, genes within the same phylogenetic subgroup exhibit distinct transcript profiles (Dubos et al., 2010). Such was the case for subgroup S14: the members in this subgroup were detected in RNA-seq-based clusters 1, 3 and 6. In *A. thaliana*, members of S14 were generally related to axillary bud formation and cell differentiation. In some cases, however, genes belonging to the same subgroups might also have similar transcription profiles in the same tissue, organ or cell type. Such was the case with the TPSA subgroup; all were present in RNA-seq-based cluster 3. Likewise, all members of subgroup S5 gathered in cluster 5.

Previous reports have pointed out that most of the genes involved in flavonoid formation and catechin biosynthesis were preferentially expressed in apical buds and young leaves, where most galloylated catechins accumulate (Wei et al., 2018). Accordingly, *R2R3-MYB*s in RNA-seq-based cluster 5, whose expression level was highest in these two tender tissues, are the most likely candidates regulating catechin biosynthesis. As is shown in Fig. 5, almost half of the genes found in cluster 5 (9) belonged to the subgroups that specifically evolved in or expanded in *C. sinensis,* subgroups S5, SMYB5, TPSB and TPSC. It is worth noting that genes of subgroup S5 and SMYB5 were confirmed to be involved in flavonoid formation in *A. thaliana* (Nesi et al., 2001; Stracke et al., 2001), whereas subgroup TPSB was inferred to be relevant to UV protection and subgroup TPSC to control plant epidermal cell fate specification.

In silico analysis of R2R3-MYB expression and catechin accumulation

Catechins are the major type of polyphenols, comprising up to 70% of the polyphenols in the tea plant. Fig 6B shows that catechin contents, especially the contents of the galloylated catechins EGCG and ECG, are significantly higher in apical buds and young leaves than in other tissues. Therefore, for understanding the possible correlation between the galloylated catechins and the *CsR2R3-MYB*s that specifically evolved or expanded in *C. sinensis*, we focused on the nine *R2R3-MYB*s grouped in cluster 5 (*CsMYB22*, *CsMYB29*, *CsMYB30*, *CsMYB31*, *CsMYB32*, *CsMYB34*, *CsMYB37*, *CsMYB39* and *CsMYB42*) because they were preferentially expressed in apical buds and young leaves.

Further, the transcript abundance of the nine potential *R2R3-MYB* TFs and the catechin biosynthesis genes were investigated in different tissues. The results clearly showed that the genes in the catechin biosynthesis pathway display tissue-specific expression patterns. The genes downstream of catechin biosynthesis (*CsSCPL1A7*, *CsANR*, *CsLAR, CsDFR, CsFLS*, *CsF3H*, *CsF3'5'H)* were highly expressed in apical buds and young leaves, whereas the upstream genes (*CsPAL*, *Cs4CL, CsC4H*) were highly expressed in root and flower (Fig. 6C). Interestingly, the nine candidate *R2R3-MYB* TFs showed preferential expression in apical buds and young leaves, which was consistent with the expression pattern of the downstream catechin biosynthetic genes, indicating that those *R2R3-MYB*s have relevance to catechin biosynthesis.

To identify the relationship between transcript abundance and catechin contents, a comprehensive gene-to-metabolite correlation analysis was conducted. As shown in Fig. 6D, the three genes in the catechin biosynthesis pathway (*CsPAL*, *CsC4H* and *Cs4CL*) that were not tender parts-specific indeed showed a low correlation or negatively correlated to catechin content. Comparatively, the expression level of the nine candidate *R2R3-MYB* TFs was positively correlated to the transcript abundance patterns of the catechin biosynthesis pathway downstream genes (*CsSCPL1A7*, *CsANR*, *CsLAR, CsDFR, CsFLS*, *CsF3H*, *CsF3'5'H)* and correlated with the contents of EGCG and ECG, with inter-gene-to-metabolite Pearson's correlation coefficients over 0.55. *CsMYB30*, *CsMYB34*, *CsMYB37* and *CsMYB42* exhibited good performance compared with the others, each having a correlation coefficient exceeding 0.75, indicating an extremely strong correlation. Notably, *CsMYB34* had the strongest correlation with the catechin biosynthesis pathway downstream genes

(>0.9), especially with *CsSCPL1A7* (0.99). Besides that, the coefficients between *CsMYB34* and EGCG and ECG contents were 0.89 and 0.86, respectively.

Validation of the correlation between *R2R3-MYB* TFs and catechins

To validate the relationship between *R2R3-MYB* TFs and catechins, HPLC and qRT-PCR assays were carried out. Different tissues of the tea plant were tested for the contents of different catechin monomers via HPLC (Fig.7A). As shown in Fig.7A, there was a high level of EGCG in all tested tissues compared with the other catechin monomers, reaching the highest level in apical buds (AB) and young leaves (FL and SL). Additionally, the expression patterns of the nine specially evolved and expanded candidate *CsR2R3-MYB*s and catechin biosynthesis genes in different tissues were verified by qRT-PCR. According to the relative expression patterns, there were four distinct clusters (cluster A-D) (Fig. 7B). The genes upstream of catechin biosynthesis (*CsPAL*, *CsC4H*, *Cs4CL*) grouped in cluster A and were highly expressed in roots, consistent with the absence of catechins in roots (Fig. 6C). *CsMYB22*, *CsMYB31* and *CsMYB42* (cluster B) had distinctly high expression in old leaves, and were not apical bud- or young leaf-specific. Remarkably, *CsMYB30*, *CsMYB32*, *CsMYB34* and *CsMYB37,* which clustered with critical genes downstream of catechins biosynthesis (cluster D) were highly expressed in apical buds and first leaves, where EGCG and ECG accumulated (Fig. 7A), preliminarily validating the intimate correlation between *CsMYB30*, *CsMYB32*, *CsMYB34*, *CsMYB37* and catechin biosynthesis.

For further confirmation, gene-to-metabolite correlation analysis of *CsMYB30*, *CsMYB32*, *CsMYB34*, *CsMYB37*, key genes of the catechin biosynthesis pathway, and the accumulation of catechins was conducted (Fig.7C). The results confirmed the extremely low correlation between four of the candidate TFs and the genes upstream of catechin biosynthesis *CsPAL*, *CsC4H* and *Cs4CL*. In contrast, *CsMYB30*, *CsMYB34* and *CsMYB37* were strongly associated with most of the major genes downstream of the galloylated catechin biosynthesis pathway (*CsSCPL1A7*, *CsANR, CsLAR* and *CsDFR*) as well as ECG and EGCG contents (> 0.7). Particularly, *CsMYB37* showed the highest correlation level with the highest inter-correlation coefficients within the four major functional genes *CsSCPL1A7*, *CsANR*, *CsLAR, CsDFR* and the contents of EGCG and ECG reaching to 0.79, 0.78, 0.88, 0.85, 0.87 and 0.8, respectively. However, *CsMYB30*, *CsMYB34* and

348 *CsMYB37* were less related to the other downstream catechin biosynthesis genes (*CsFLS*, *CsF3H*,
349 *CsF3'5'H*) according to their lower Pearson's correlation coefficients. Consistent with the *in silico*
350 results in Fig. 6D, the correlation among *CsMYB32*, the galloylated catechin contents and the
351 biosynthesis genes was weaker than the other three *R2R3-MYB*s. In more detail, it had a relatively
352 low correlation coefficient with ECG (0.52) and EGCG (0.67), and a relatively low correlation
353 coefficient with genes *CsSCPL1A, CsANR, CsLAR* and *CsDFR* (0.5, 0.36, 0.74 and 0.37,
354 respectively).

355 The results provide convincing clues that *CsMYB30*, *CsMYB34*, *CsMYB37* might be the key
356 transcription factors regulating galloylated catechins biosynthesis for the *Camellia*-specific
357 specialized metabolites ECG and EGCG.

358

359 **Discussion**

360 Plants are rich in metabolites that allow them to adapt to the environment and resist biotic and
361 abiotic stress (Howe and Jander, 2008). These metabolites are widely used as natural products for
362 treating human diseases and are valuable raw materials for modern industry (Guo et al., 2018; Fang
363 et al., 2019; Howe et al., 2008; Plomion et al., 2001). *C. sinensis* is an advantageous model system
364 to dig into plant-specific metabolite biosynthesis and genetic regulation. Its metabolites, such as
365 flavonoids, caffeine, and volatile terpenes, accumulate in abundance and share characteristics with
366 the same metabolites in other plant lineages (Yu et al., 2020).

367 Galloylated catechins are secondary metabolites only found in *Vitis vinifera* and *C. sinensis* (Wei
368 et al., 2018). Contrary to the small amount of galloylated catechins present in the form of ECG in
369 *Vitis vinifera* (Bontpart et al., 2018), they are abundant in *C. sinensis*, and EGCG, only existing in
370 tea plants, is the predominant form (Kim et al., 2004; Steinmann et al., 2013). It is the most bioactive
371 component among the catechin enantiomers, and is derived from the flavonoid branch of the
372 phenylpropanoid metabolite pathway. The acyltransferase family, belonging to subclade 1A of
373 serine carboxypeptidase-like (SCPL) acyltransferases, acts as the most critical downstream gene
374 family involved in the production of EGCG and ECG (Wei et al., 2018). This family extensively

375 expanded to 22 members in the *C. sinensis* genome, while the *Vitis vinifera* genome contains half
376 that number (11) (Wei et al., 2018). Two key enzymes Epicatechin:1-O-galloyl-b-D-glucose O-
377 galloyltransferase (ECGT) and UDP-glucose: galloyl-1-O-b-D-glucosyltransferase (UGGT) are
378 recruited to catalyze the last two reactions in this bioprocess (Liu et al., 2012). The biosynthesis of
379 galloylated catechins in *C. sinensis* has been comprehensively investigated with regard to the
380 biosynthesis genes of the pathway. However, the transcriptional regulation of these pathways
381 remains to be illuminated.

382 Genes responsible for plant secondary metabolite biosynthesis are coordinately regulated by TFs,
383 a regulatory superfamily that dynamically drives the evolution of plant metabolic pathways for
384 special compounds (Shoji et al., 2021). The regulatory network of this gene superfamily is highly
385 conserved both in angiosperms and gymnosperms (Zhang et al., 2014). The *R2R3-MYB* TFs confer
386 tissue-specific or development stage-specific patterns for metabolites in the same biosynthesis
387 pathway; often, multiple paralogues coexist in one species (Zhang et al., 2014). Lignin, flavonoids,
388 anthocyanins and capsaicinoids are four different types of secondary metabolites synthesized from
389 the phenylpropanoid pathway that are regulated by *R2R3-MYB* TFs (Sun et al., 2016; Zhu et al.,
390 2019; Soler et al., 2015). Remarkably, the great expansion of this transcription-regulatory
391 superfamily in plant lineages appears to account for the diversity of regulatory functions that the
392 *R2R3-MYB* TFs undertake in plant-specific metabolic bioprocesses (Millard et al., 2019). As
393 demonstrated in detail by the analysis of Soler et.al, the R2R3-MYB subgroups in *E. grandis*, *V.*
394 *vinifera* and *P. trichocarpa*, which were equipped with expanded members, greatly determined the
395 diversification of specific functions in lignin biosynthesis (Soler et al., 2015).

396 Based on the consideration of the unique and abundant accumulation of the specific galloylated
397 catechins (ECG and EGCG) in tea plant and tea-specific *R2R3-MYB* TFs identified in this work, we
398 hypothesize that the biosynthesis of the characteristic galloylated catechins is absolutely influenced
399 at the transcription regulation level. Different from the result that concentrates on the involvement
400 of some *CsR2R3-MYB* genes in response to drought, cold, gibberellic acid (GA), and abscisic acid
401 (ABA) treatments, which are revealed in the recent genome-wide report of this family(Chen et al.,
402 2021), we firstly emphasize on confirming the putative *R2R3-MYB* candidates that directly function

in the production of *Camellia*-specialized compounds (EGCG) among the tea-specific *R2R3-MYB* transcription factors.

The comprehensive and comparative phylogenetic analysis of *CsR2R3-MYB* TFs, backed by multiple sequence alignment among *C. sinensis* and *A. thaliana,* suggests that most of the members in this family are conserved. Most *R2R3-MYB*s share similar functions to the homologous counterparts studied in *A. thaliana*. Some of the *R2R3-MYB* TFs that clustered in TPSA, TPSB and TPSC subgroups evolved exclusively in *C. sinensis*, but have isogenous genes in *Actinidia chinensis*, *Vitis vinifera*, *Theobroma cacao* and *Coffea canephora* genomes. Thus, we speculated that TPSA, TPSB and TPSC are either obtained in *C. sinensis* or lost in *A. thaliana* lineages after divergence from their most recent common ancestor during two whole-genome duplication (WGD) events. In addition, members of SMYB5 and S5 subgroups, regulating flavonoids biosynthesis in *A. thaliana*, are greatly expanded in *C. sinensis*, which suggests that they might be either functionally redundant genes or genes that undertake some novel functions in the tea plant.

Considering that characteristic catechins highly accumulate in apical buds and young leaves, we speculated that the *CsR2R3-MYB* TFs that are preferentially expressed in these tender tissues along with the major catechin-biosynthesis genes are the most promising candidates putatively regulating the biosynthesis of tea-specific catechins. Consistent with previous results (Wei et al., 2018), our study observed high expression levels of key galloylated catechin biosynthesis genes *SCPL1A, ANR, LAR* and *DFR* in tender tissues, while the expression of upstream genes (*PAL*, *C4H*, *4CL*) in the phenylpropanoid pathway that are mainly relevant to the generation of condensed polymer proanthocyanidins (PAs), was in fruits, flowers and roots. However, *CsMYB42* was preferentially expressed in tender tissues and had a strong correlation with catechin biosynthesis genes and the contents of ECG and EGCG in the 'Shuchazao' variety (Fig. 6D), while it was preferentially expressed in old leaves in the 'Lingtoudancong' variety (Fig. 7C). Thus, differences can be observed in different *C. sinensis* varieties. Eventually, through systematic analyses, *CsMYB30* (TPSC subgroup), *CsMYB34* (S5 subgroup) and *CsMYB37* (SMYB5 subgroup) were confirmed as the potential *R2R3-MYB* TFs relevant to the internal accumulation of characteristic catechins (ECG and EGCG) in *C. sinensis*, however, further investigation is needed. This study laid a theoretical

framework and valuable foundation for the needed future work, as we have provided a considerable amount of preliminarily evidence through systematic bioinformatics analysis to gain a deeper perception of the functional roles of the R2R3-MYB superfamily in *C. sinensis*. Nevertheless, it is still necessary to further exploration and validate these results.

Conclusions

A total of 118 *R2R3-MYB* gene members, classified into 38 subgroups, were identified in the *C. sinensis* genome. Notably, five subgroups (TPSA, TPSB, TPSC, S5 and SMYB5) containing 21 *R2R3-MYB* TFs were identified to be remarkably expanded in or completely unique to *C. sinensis*. Furthermore, gene structure predictions, expression profile validation and correlation analyses were subsequently conducted to screen out the most promising candidate *R2R3-MYB* TFs (*CsMYB30*, *CsMYB34* and *CsMYB37*) that positively function in galloylated catechin biosynthesis in tea plants. The present findings underpin a basic understanding of species-specific regulatory mechanisms that *C. sinensis* employs to biosynthesize specialized metabolites and will be beneficial for selecting favorable *C. sinensis* germplasms.

Abbreviation

C, catechin; EC, epicatechin; GC, gallatechin; EGC, epigallocatechin; CG, catechin gallate; ECG, epigallocatechin gallate; GCG, gallatechin gallate; EGCG, epigallocatechin gallate; qRT-PCR, Quantitative reverse transcription polymerase chain reaction; PAL, Phenylalanine ammonia lyase; C4H, Cinnamate 4-hydroxylase; 4CL, 4-Coumarate: coenzyme A ligase; CHS, Chalcone synthase; CHI, Chalcone isomerase; F3H, Flavanone -3-hydroxylase; F3'H, Flavonoid 3'-hydroxylase; F3'5'H, Flavonoid 3'5'-hydroxylase; FLS, Flavonol synthase; DFR, Dihydroflavonol 4-reductase; ANS, Anthocyanidin synthase; ANR, Anthocyanidin reductase; LAR, Leucoanthcyanidin 4-reductase; SCPL1A, Subclade 1A of serine carboxypeptidase-like acyltransferases; TFs, transcription factors; HPLC, high-performance liquid chromatography; Trp/W, tryptophan.

Data availablity statement

The original contributions presented in the study are included in the article/Supplementary Material, further inquiries can be directed to the corresponding author/s.

Authors' contributions

J.L. performed the qRT-PCR test, analyzed the data, made the data charts and wrote the manuscript. S.L. conceived the project and supervised the researches. P.C. carried out the HPLC test. J.C., S.T. and W.Y collected the materials for the experiments and provided useful suggestions. F.C. reviewed and edited the manuscript. P.Z funded the researches and reviewed the manuscript. B.S. designed the project, supervised the researches, interpreted data and edited the manuscript.

Conflicts of interest

The authors declare that they have no conflicts of interest with the contents of this article.

Funding

This work was supported by the Natural Science Foundation of Guangdong Province (2021A1515012091) and the Science and Technology Projects of Guangzhou (202102020290).

Appendix A. Supplementary data

References

Abbas, M., Saeed, F., Anjum, F.M., Afzaal, M., Tufail, T., Bashir, M.S., Ishtiaq, A., Hussain, S., Suleria, H.A.R., 2017. Natural polyphenols: An overview. Int. J. Food Prop. 20, 1689–1699. https://doi.org/10.1080/10942912.2016.1220393

482 Ahmad, N., Feyes, D.K., Agarwal, R., Mukhtar, H., Nieminen, A.-L., 1997. Green tea constituent
483 epigallocatechin-3-gallate and induction of apoptosis and cell cycle arrest in human
484 carcinoma cells. JNCI J. Natl. Cancer Inst. 89, 1881–1886.
485 https://doi.org/10.1093/jnci/89.24.1881

486 Ahmad, N., Gupta, S., Mukhtar, H., 2000. Green tea polyphenol epigallocatechin-3-gallate
487 differentially modulates nuclear factor κB in cancer cells versus normal cells. Arch.
488 Biochem. Biophys. 376, 338–346. https://doi.org/10.1006/abbi.2000.1742

489 Ambawat, S., Sharma, P., Yadav, N.R., Yadav, R.C., 2013. MYB transcription factor genes as
490 regulators for plant responses: an overview. Physiol. Mol. Biol. Plants 19, 307–321.
491 https://doi.org/10.1007/s12298-013-0179-1

492 Asakawa, T., Hamashima, Y., Kan, T., 2013. Chemical synthesis of tea polyphenols and related
493 compounds. Curr. Pharm. Des. 19, 6207–6217.
494 https://doi.org/10.2174/1381612811319340012

495 Ashihara, H., Deng, W.-W., Mullen, W., Crozier, A., 2010. Distribution and biosynthesis of
496 flavan-3-ols in *Camellia sinensis* seedlings and expression of genes encoding biosynthetic
497 enzymes. Phytochemistry 71, 559–566.
498 https://doi.org/https://doi.org/10.1016/j.phytochem.2010.01.010

499 Bailey, T.L., Boden, M., Buske, F.A., Frith, M., Grant, C.E., Clementi, L., Ren, J., Li, W.W.,
500 Noble, W.S., 2009. MEME Suite: Tools for motif discovery and searching. Nucleic Acids
501 Res. 37, 202–208. https://doi.org/10.1093/nar/gkp335

502 Bedon, F., Grima-Pettenati, J., Mackay, J., 2007. Conifer R2R3-MYB transcription factors:
503 sequence analyses and gene expression in wood-forming tissues of white spruce (Picea
504 glauca). BMC Plant Biol. 7, 17. https://doi.org/10.1186/1471-2229-7-17

505 Bontpart, T., Ferrero, M., Khater, F., Marlin, T., Vialet, S., Vallverdù-Queralt, A., Pinasseau, L.,
506 Ageorges, A., Cheynier, V., Terrier, N., 2018. Focus on putative serine carboxypeptidase-
507 like acyltransferases in grapevine. Plant Physiol. Biochem. 130, 356–366.

508 https://doi.org/10.1016/j.plaphy.2018.07.023

509 Cao, Z.-H., Zhang, S.-Z., Wang, R.-K., Zhang, R.-F., Hao, Y.-J., 2013. Genome wide analysis of
510 the apple MYB transcription factor family allows the identification of *MdoMYB121* gene
511 confering abiotic stress tolerance in plants. PLoS One 8, e69955.
512 https://doi.org/10.1371/journal.pone.0069955

513 Chen, C., Chen, H., Zhang, Y., Thomas, H.R., Frank, M.H., He, Y., Xia, R., 2020. TBtools: An
514 integrative toolkit developed for interactive analyses of big biological data. Mol. Plant 13,
515 1194–1202. https://doi.org/10.1016/j.molp.2020.06.009

516 Chen, X., Wang, P., Gu, M., Lin, X., Hou, B., Zheng, Y., Sun, Y., Jin, S., Ye, N., 2021. R2R3-
517 MYB transcription factor family in tea plant (*Camellia sinensis*): Genome-wide
518 characterization, phylogeny, chromosome location, structure and expression patterns.
519 Genomics 113, 1565–1578. https://doi.org/10.1016/j.ygeno.2021.03.033

520 Chen, Y., Yu, M., Xu, J., Chen, X., Shi, J., 2009. Differentiation of eight tea (*Camellia sinensis*)
521 cultivars in China by elemental fingerprint of their leaves. J. Sci. Food Agric. 89, 2350–
522 2355. https://doi.org/10.1002/jsfa.3716

523 Cheng, Y., Zhu, W., Chen, Y., Ito, S., Asami, T., Wang, X., 2014. Brassinosteroids control root
524 epidermal cell fate via direct regulation of a MYB-bHLH-WD40 complex by GSK3-like
525 kinases. Elife 3. https://doi.org/10.7554/eLife.02525

526 Drew, B., 2019. The growth of tea. Nature 566, S2-S4. https://doi.org/10.1038/d41586-019-
527 00395-4

528 Du, H., Yang, S.-S., Liang, Z., Feng, B.-R., Liu, L., Huang, Y.-B., Tang, Y.-X., 2012. Genome-
529 wide analysis of the MYB transcription factor superfamily in soybean. BMC Plant Biol. 12,
530 106. https://doi.org/10.1186/1471-2229-12-106

531 Dubos, C., Stracke, R., Grotewold, E., Weisshaar, B., Martin, C., Lepiniec, L., 2010. MYB
532 transcription factors in *Arabidopsis*. Trends Plant Sci. 15, 573–581.
533 https://doi.org/10.1016/j.tplants.2010.06.005

534 Eungwanichayapant, P.D., Popluechai, S., 2009. Accumulation of catechins in tea in relation to
535 accumulation of mRNA from genes involved in catechin biosynthesis. Plant Physiol.
536 Biochem. 47, 94–97. https://doi.org/https://doi.org/10.1016/j.plaphy.2008.11.002

537 Fang, C., Fernie, A.R., Luo, J., 2019. Exploring the diversity of plant metabolism. Trends Plant
538 Sci. 24, 83–98. https://doi.org/https://doi.org/10.1016/j.tplants.2018.09.006

539 Fukai, K., Ishigami, T., Hara, Y., 1991. Antibacterial activity of tea polyphenols against
540 phytopathogenic bacteria. Agric. Biol. Chem. 55, 1895–1897.
541 https://doi.org/10.1080/00021369.1991.10870886

542 Gigolashvili, T., Yatusevich, R., Berger, B., Müller, C., Flügge, U.-I., 2007. The R2R3-MYB
543 transcription factor *HAG1/MYB28* is a regulator of methionine-derived glucosinolate
544 biosynthesis in *Arabidopsis thaliana*. Plant J. 51, 247–261. https://doi.org/10.1111/j.1365-
545 313X.2007.03133.x

546 Goicoechea, M., Lacombe, E., Legay, S., Mihaljevic, S., Rech, P., Jauneau, A., Lapierre, C.,
547 Pollet, B., Verhaegen, D., Chaubet-Gigot, N., Grima-Pettenati, J., 2005. *EgMYB2*, a new
548 transcriptional activator from Eucalyptus xylem, regulates secondary cell wall formation and
549 lignin biosynthesis. Plant J. 43, 553–567. https://doi.org/https://doi.org/10.1111/j.1365-
550 313X.2005.02480.x

551 Gonzalez, A., Mendenhall, J., Huo, Y., Lloyd, A., 2009. *TTG1* complex MYBs, *MYB5* and *TT2*,
552 control outer seed coat differentiation. Dev. Biol. 325, 412–421.
553 https://doi.org/https://doi.org/10.1016/j.ydbio.2008.10.005

554 Guo, L., Winzer, T., Yang, X., Li, Y., Ning, Z., He, Z., Teodor, R., Lu, Y., Bowser, T.A., Graham,
555 I.A., Ye, K., 2018. The opium poppy genome and morphinan production. Science 362, 343–
556 347. https://doi.org/10.1126/science.aat4096

557 He, X., Zhao, X., Gao, L., Shi, X., Dai, X., Liu, Y., Xia, T., Wang, Y., 2018. Isolation and
558 characterization of key genes that promote flavonoid accumulation in purple-leaf tea
559 (C*amellia sinensis* L.). Sci. Rep. 8, 1–13. https://doi.org/10.1038/s41598-017-18133-z

560 Heim, K.E., Tagliaferro, A.R., Bobilya, D.J., 2002. Flavonoid antioxidants: chemistry, metabolism
561 and structure-activity relationships. J. Nutr. Biochem. 13, 572–584.
562 https://doi.org/10.1016/s0955-2863(02)00208-5

563 Hichri, I., Barrieu, F., Bogs, J., Kappel, C., Delrot, S., Lauvergeat, V., 2011. Recent advances in
564 the transcriptional regulation of the flavonoid biosynthetic pathway. J. Exp. Bot. 62, 2465–
565 2483. https://doi.org/10.1093/jxb/erq442

566 Howe, G.A., Jander, G., 2008. Plant immunity to insect herbivores. Annu. Rev. Plant Biol. 59, 41–
567 66. https://doi.org/10.1146/annurev.arplant.59.032607.092825

568 Jiang, C., Gu, X., Peterson, T., 2004. Identification of conserved gene structures and carboxy-
569 terminal motifs in the Myb gene family of *Arabidopsis* and *Oryza sativa* L. ssp. *indica*.
570 Genome Biol. 5, R46. https://doi.org/10.1186/gb-2004-5-7-r46

571 Jin, H., Martin, C., 1999. Multifunctionality and diversity within the plant MYB-gene family.
572 Plant Mol. Biol. 41, 577–585. https://doi.org/10.1023/a:1006319732410

573 Jiu, S., Guan, L., Leng, X., Zhang, K., Haider, M.S., Yu, X., Zhu, X., Zheng, T., Ge, M., Wang,
574 C., Jia, H., Shangguan, L., Zhang, C., Tang, X., Abdullah, M., Javed, H.U., Han, J., Dong,
575 Z., Fang, J., 2021. The role of *VvMYBA2r* and *VvMYBA2w* alleles of the *MYBA2* locus in the
576 regulation of anthocyanin biosynthesis for molecular breeding of grape (*Vitis* spp.) skin
577 coloration. Plant Biotechnol. J. 19, 1216–1239. https://doi.org/10.1111/pbi.13543

578 Kim, S.Y., Ahn, B.H., Min, K.J., Lee, Y.H., Joe, E.H., Min, D.S., 2004. Phospholipase D
579 isozymes mediate epigallocatechin gallate-induced cyclooxygenase-2 expression in astrocyte
580 cells. J. Biol. Chem. 279, 38125. https://doi.org/10.1074/jbc.M402085200

581 Kranz, H.D., Denekamp, M., Greco, R., Jin, H., Leyva, A., Meissner, R.C., Petroni, K., Urzainqui,
582 A., Bevan, M., Martin, C., Smeekens, S., Tonelli, C., Paz-Ares, J., Weisshaar, B., 1998.
583 Towards functional characterisation of the members of the *R2R3-MYB* gene family from
584 *Arabidopsis thaliana*. Plant J. 16, 263–276. https://doi.org/10.1046/j.1365-
585 313x.1998.00278.x

586 Kumar, S., Stecher, G., Tamura, K., 2016. MEGA7: Molecular evolutionary genetics analysis
587 version 7.0 for bigger datasets. Mol. Biol. Evol. 33, 1870–1874.
588 https://doi.org/10.1093/molbev/msw054

589 Li, M., Li, Y., Guo, L., Gong, N., Pang, Y., Jiang, W., Liu, Y., Jiang, X., Zhao, L., Wang, Y., Xie,
590 D.-Y., Gao, L., Xia, T., 2017. Functional characterization of tea (*Camellia sinensis*) *MYB4a*
591 transcription factor using an integrative approach. Front. Plant Sci. 8, 943.
592 https://doi.org/10.3389/fpls.2017.00943

593 Li, S., Sun, L., Fan, X., Zhang, Y., Jiang, J., Liu, C., 2020. Functional analysis of *Vitis davidii*
594 R2R3-MYB transcription factor *VdMYB14* in the regulation of flavonoid biosynthesis. J.
595 Fruit Sci. 37, 783–792. https://doi.org/10.13925/j.cnki.gsxb.20190577

596 Li, W., Ding, Z., Ruan, M., Yu, X., Peng, M., Liu, Y., 2017. Kiwifruit R2R3-MYB transcription
597 factors and contribution of the novel *AcMYB75* to red kiwifruit anthocyanin biosynthesis.
598 Sci. Rep. 7, 16861. https://doi.org/10.1038/s41598-017-16905-1

599 Li, X., Xue, C., Li, J., Qiao, X., Li, L., Yu, L., Huang, Y., Wu, J., 2016. Genome-wide
600 identification, evolution and functional divergence of MYB transcription factors in Chinese
601 White Pear (*Pyrus bretschneideri*). Plant Cell Physiol. 57, 824–847.
602 https://doi.org/10.1093/pcp/pcw029

603 Lipsick, J.S., 1996. One billion years of Myb. Oncogene 13, 223–235.

604 Liu, Y., Gao, L., Liu, L., Yang, Q., Lu, Z., Nie, Z., Wang, Y., Xia, T., 2012. Purification and
605 characterization of a novel galloyltransferase involved in catechin galloylation in the tea
606 plant (*Camellia sinensis*)*. J. Biol. Chem. 287, 44406–44417.
607 https://doi.org/https://doi.org/10.1074/jbc.M112.403071

608 Livak, K.J., Schmittgen, T.D., 2001. Analysis of relative gene expression data using real-time
609 quantitative PCR and the 2(-Delta Delta C(T)) Method. Methods 25, 402–408.
610 https://doi.org/10.1006/meth.2001.1262

611 Martin, C., Paz-Ares, J., 1997. MYB transcription factors in plants. Trends Genet. 13, 67–73.

612 https://doi.org/https://doi.org/10.1016/S0168-9525(96)10049-4

613 Matus, J.T., Aquea, F., Arce-Johnson, P., 2008. Analysis of the grape MYB R2R3 subfamily
614 reveals expanded wine quality-related clades and conserved gene structure organization
615 across *Vitis* and *Arabidopsis* genomes. BMC Plant Biol. 8, 83. https://doi.org/10.1186/1471-
616 2229-8-83

617 Mehrtens, F., Kranz, H., Bednarek, P., Weisshaar, B., 2005. The *Arabidopsis* transcription factor
618 MYB12 is a flavonol-specific regulator of phenylpropanoid biosynthesis. Plant Physiol.
619 138, 1083–1096. https://doi.org/10.1104/pp.104.058032

620 Millard, P.S., Kragelund, B.B., Burow, M., 2019. R2R3 MYB transcription factors – functions
621 outside the DNA-binding domain. Trends Plant Sci. 24, 934–946.
622 https://doi.org/https://doi.org/10.1016/j.tplants.2019.07.003

623 Mondal, T.K., Bhattacharya, A., Laxmikumaran, M., Ahuja, P.S., 2004. Recent advances of tea
624 (*Camellia sinensis*) biotechnology. Plant Cell. Tissue Organ Cult. 76, 195–254.
625 https://doi.org/10.1023/B:TICU.0000009254.87882.71

626 Nesi, N., Jond, C., Debeaujon, I., Caboche, M., Lepiniec, L., 2001. The *Arabidopsis TT2* gene
627 encodes an R2R3 MYB domain protein that acts as a key determinant for proanthocyanidin
628 accumulation in developing seed. Plant Cell 13, 2099–2114.
629 https://doi.org/10.1105/tpc.010098

630 Nikoo, M., Regenstein, J.M., Ahmadi Gavlighi, H., 2018. Antioxidant and antimicrobial activities
631 of (-)-epigallocatechin-3-gallate (EGCG) and its potential to preserve the quality and safety
632 of foods. Compr. Rev. Food Sci. Food Saf. 17, 732–753. https://doi.org/10.1111/1541-
633 4337.12346

634 Ogata, K., Morikawa, S., Nakamura, H., Hojo, H., Yoshimura, S., Zhang, R., Aimoto, S.,
635 Ametani, Y., Hirata, Z., Sarai, A., Ishii, S., Nishimura, Y., 1995. Comparison of the free and
636 DNA-complexed forms of the DMA-binding domain from c-Myb. Nat. Struct. Biol. 2, 309–
637 320. https://doi.org/10.1038/nsb0495-309

638 Park, M.-R., Yun, K.-Y., Mohanty, B., Herath, V., Xu, F., Wijaya, E., Bajic, V.B., Yun, S.-J., De
639 Los Reyes, B.G., 2010. Supra-optimal expression of the cold-regulated OsMyb4
640 transcription factor in transgenic rice changes the complexity of transcriptional network
641 with major effects on stress tolerance and panicle development. Plant. Cell Environ. 33,
642 2209–2230. https://doi.org/10.1111/j.1365-3040.2010.02221.x

643 Patzlaff, A., McInnis, S., Courtenay, A., Surman, C., Newman, L.J., Smith, C., Bevan, M.W.,
644 Mansfield, S., Whetten, R.W., Sederoff, R.R., Campbell, M.M., 2003. Characterisation of a
645 pine MYB that regulates lignification. Plant J. 36, 743–754.
646 https://doi.org/https://doi.org/10.1046/j.1365-313X.2003.01916.x

647 Plomion, C., Leprovost, G., Stokes, A., 2001. Wood formation in trees. Plant Physiol. 127, 1513–
648 1523. https://doi.org/10.1104/pp.010816

649 Punyasiri, P.A.N., Abeysinghe, I.S.B., Kumar, V., Treutter, D., Duy, D., Gosch, C., Martens, S.,
650 Forkmann, G., Fischer, T.C., 2004. Flavonoid biosynthesis in the tea plant *Camellia*
651 *sinensis*: properties of enzymes of the prominent epicatechin and catechin pathways. Arch.
652 Biochem. Biophys. 431, 22–30. https://doi.org/https://doi.org/10.1016/j.abb.2004.08.003

653 Sakanaka, S., Juneja, L.R., Taniguchi, M., 2000. Antimicrobial effects of green tea polyphenols on
654 thermophilic spore-forming bacteria. J. Biosci. Bioeng. 90, 81–85.
655 https://doi.org/10.1016/s1389-1723(00)80038-9

656 Savage, N., Yang, T.J.W., Chen, C.Y., Lin, K.-L., Monk, N.A.M., Schmidt, W., 2013. Positional
657 signaling and expression of *ENHANCER OF TRY AND CPC1* are tuned to increase root
658 hair density in response to phosphate deficiency in *Arabidopsis thaliana*. PLoS One 8,
659 e75452. https://doi.org/10.1371/journal.pone.0075452

660 Schenke, D., Cai, D., Scheel, D., 2014. Suppression of UV-B stress responses by flg22 is
661 regulated at the chromatin level via histone modification. Plant. Cell Environ. 37, 1716–
662 1721. https://doi.org/10.1111/pce.12283

663 Shoji, T., Umemoto, N., Saito, K., 2021. Genetic divergence in transcriptional regulators of

664 defense metabolism: insight into plant domestication and improvement. Plant Mol. Biol.
665 https://doi.org/10.1007/s11103-021-01159-3

666 Singh, K., Kumar, S., Rani, A., Gulati, A., Ahuja, P.S., 2009a. Phenylalanine ammonia-lyase
667 (PAL) and cinnamate 4-hydroxylase (C4H) and catechins (flavan-3-ols) accumulation in
668 tea. Funct. Integr. Genomics 9, 125–134. https://doi.org/10.1007/s10142-008-0092-9

669 Singh, K., Rani, A., Kumar, S., Sood, P., Mahajan, M., Yadav, S.K., Singh, B., Ahuja, P.S., 2008.
670 An early gene of the flavonoid pathway, flavanone 3-hydroxylase, exhibits a positive
671 relationship with the concentration of catechins in tea (*Camellia sinensis*). Tree Physiol. 28,
672 1349–1356. https://doi.org/10.1093/treephys/28.9.1349

673 Singh, K., Rani, A., Paul, A., Dutt, S., Joshi, R., Gulati, A., Ahuja, P.S., Kumar, S., 2009b.
674 Differential display mediated cloning of anthocyanidin reductase gene from tea (*Camellia*
675 *sinensis*) and its relationship with the concentration of epicatechins. Tree Physiol. 29, 837–
676 846. https://doi.org/10.1093/treephys/tpp022

677 Soler, M., Camargo, E.L.O., Carocha, V., Cassan-Wang, H., San Clemente, H., Savelli, B., Hefer,
678 C.A., Paiva, J.A.P., Myburg, A.A., Grima-Pettenati, J., 2015. The eucalyptus grandis R2R3-
679 MYB transcription factor family: Evidence for woody growth-related evolution and
680 function. New Phytol. 206, 1364–1377. https://doi.org/10.1111/nph.13039

681 Steinmann, J., Buer, J., Pietschmann, T., Steinmann, E., 2013. Anti-infective properties of
682 epigallocatechin-3-gallate (EGCG), a component of green tea. Br. J. Pharmacol. 168, 1059–
683 1073. https://doi.org/10.1111/bph.12009

684 Stracke, R., Werber, M., Weisshaar, B., 2001. The R2R3-MYB gene family in *Arabidopsis*
685 *thaliana*. Curr. Opin. Plant Biol. 4, 447–456. https://doi.org/10.1016/s1369-5266(00)00199-
686 0

687 Sun, B., Zhu, Z., Cao, P., Chen, H., Chen, C., Zhou, X., Mao, Y., Lei, J., Jiang, Y., Meng, W.,
688 Wang, Y., Liu, S., 2016. Purple foliage coloration in tea (*Camellia sinensis* L.) arises from
689 activation of the R2R3-MYB transcription factor CsAN1. Sci. Rep. 6.

https://doi.org/10.1038/srep32534

Surh, Y.-J., 2003. Cancer chemoprevention with dietary phytochemicals. Nat. Rev. Cancer 3, 768–780. https://doi.org/10.1038/nrc1189

Taguri, T., Tanaka, T., Kouno, I., 2004. Antimicrobial activity of 10 different plant polyphenols against bacteria causing food-borne disease. Biol. Pharm. Bull. 27, 1965–1969. https://doi.org/10.1248/bpb.27.1965

Teng, S., Keurentjes, J., Bentsink, L., Koornneef, M., Smeekens, S., 2005. Sucrose-specific induction of anthocyanin biosynthesis in *Arabidopsis* requires the *MYB75/PAP1* gene. Plant Physiol. 139, 1840–1852. https://doi.org/10.1104/pp.105.066688

Velasco, R., Zharkikh, A., Troggio, M., Cartwright, D.A., Cestaro, A., Pruss, D., Pindo, M., FitzGerald, L.M., Vezzulli, S., Reid, J., Malacarne, G., Iliev, D., Coppola, G., Wardell, B., Micheletti, D., Macalma, T., Facci, M., Mitchell, J.T., Perazzolli, M., Eldredge, G., Gatto, P., Oyzerski, R., Moretto, M., Gutin, N., Stefanini, M., Chen, Y., Segala, C., Davenport, C., Dematté, L., Mraz, A., Battilana, J., Stormo, K., Costa, F., Tao, Q., Si-Ammour, A., Harkins, T., Lackey, A., Perbost, C., Taillon, B., Stella, A., Solovyev, V., Fawcett, J.A., Sterck, L., Vandepoele, K., Grando, S.M., Toppo, S., Moser, C., Lanchbury, J., Bogden, R., Skolnick, M., Sgaremella, V., Bhatnagar, S.K., Fontana, P., Gutin, A., Van de Peer, Y., Salamini, F., Viola, R., 2007. A high quality draft consensus sequence of the genome of a heterozygous grapevine variety. PLoS One 2. https://doi.org/10.1371/journal.pone.0001326

Wei, C., Yang, H., Wang, S., Zhao, J., Liu, C., Gao, L., Xia, E., Lu, Y., Tai, Y., She, G., Sun, J., Cao, H., Tong, W., Gao, Q., Li, Y., Deng, W., Jiang, X., Wang, W., Chen, Q., Zhang, S., Li, H., Wu, J., Wang, P., Li, P., Shi, C., Zheng, F., Jian, J., Huang, B., Shan, D., Shi, M., Fang, C., Yue, Y., Li, F., Li, D., Wei, S., Han, B., Jiang, C., Yin, Y., Xia, T., Zhang, Z., Bennetzen, J.L., Zhao, S., Wan, X., 2018. Draft genome sequence of *Camellia sinensis* var. *sinensis* provides insights into the evolution of the tea genome and tea quality. Proc. Natl. Acad. Sci. U. S. A. 115, E4151–E4158. https://doi.org/10.1073/pnas.1719622115

Wei, K., Wang, L., Zhang, Y., Ruan, L., Li, H., Wu, L., Xu, L., Zhang, C., Zhou, X., Cheng, H.,

717 Edwards, R., 2019. A coupled role for *CsMYB75* and *CsGSTF1* in anthocyanin
718 hyperaccumulation in purple tea. Plant J. 97, 825–840. https://doi.org/10.1111/tpj.14161

719 Wilkins, O., Nahal, H., Foong, J., Provart, N.J., Campbell, M.M., 2009. Expansion and
720 diversification of the *Populus* R2R3-MYB family of transcription factors. Plant Physiol.
721 149, 981–993. https://doi.org/10.1104/pp.108.132795

722 Yamashita, H., Uchida, T., Tanaka, Y., Katai, H., Nagano, A.J., Morita, A., Ikka, T., 2020.
723 Genomic predictions and genome-wide association studies based on RAD-seq of quality-
724 related metabolites for the genomics-assisted breeding of tea plants. Sci. Rep. 10, 17480.
725 https://doi.org/10.1038/s41598-020-74623-7

726 Yang, D., Liu, Y., Sun, M., Zhao, L., Wang, Y., Chen, X., Wei, C., Gao, L., Xia, T., 2012.
727 Differential gene expression in tea (*Camellia sinensis* L.) calli with different morphologies
728 and catechin contents. J. Plant Physiol. 169, 163–175.
729 https://doi.org/https://doi.org/10.1016/j.jplph.2011.08.015

730 Yokozawa, T., Dong, E., Nakagawa, T., Kashiwagi, H., Nakagawa, H., Takeuchi, S., Chung,
731 H.Y., 1998. In Vitro and in Vivo studies on the radical-scavenging activity of tea. J. Agric.
732 Food Chem. 46, 2143–2150. https://doi.org/10.1021/jf970985c

733 Yu, M., Man, Y., Lei, R., Lu, X., Wang, Y., 2020. Metabolomics study of flavonoids and
734 anthocyanin-related gene analysis in kiwifruit (*Actinidia chinensis*) and kiwiberry (*Actinidia*
735 *arguta*). Plant Mol. Biol. Report. 38, 353–369. https://doi.org/10.1007/s11105-020-01200-7

736 Yu, S., Li, P., Zhao, X., Tan, M., Ahmad, M.Z., Xu, Y., Tadege, M., Zhao, J., 2021. *CsTCP*s
737 regulate shoot tip development and catechin biosynthesis in tea plant (*Camellia sinensis*).
738 Hortic. Res. 8, 104. https://doi.org/10.1038/s41438-021-00538-7

739 Yu, X., Xiao, J., Chen, S., Yu, Y., Ma, J., Lin, Y., Li, R., Lin, J., Fu, Z., Zhou, Q., Chao, Q., Chen,
740 L., Yang, Z., Liu, R., 2020. Metabolite signatures of diverse *Camellia sinensis* tea
741 populations. Nat. Commun. 11, 5586. https://doi.org/10.1038/s41467-020-19441-1

742 Zhang, P., Chopra, S., Peterson, T., 2000. A segmental gene duplication generated differentially

743 expressed *myb*-homologous genes in Maize. Plant Cell 12, 2311.
744 https://doi.org/10.2307/3871231

745 Zhang, Y., Butelli, E., Martin, C., 2014. Engineering anthocyanin biosynthesis in plants. Curr.
746 Opin. Plant Biol. 19, 81–90. https://doi.org/10.1016/j.pbi.2014.05.011

747 Zhu, Z., Sun, B., Cai, W., Zhou, X., Mao, Y., Chen, Chengjie, Wei, J., Cao, B., Chen, Changming,
748 Chen, G., Lei, J., 2019. Natural variations in the MYB transcription factor *MYB31* determine
749 the evolution of extremely pungent peppers. New Phytol. https://doi.org/10.1111/nph.15853

750

751 **Annotation of figures**

752 **Figure 1**. Phylogenetic analysis of the R2R3-MYB families in *C. sinensis* and *A. thaliana*. A
753 neighbor-joining phylogenetic tree was constructed from 244 protein sequences including all R2R3-
754 MYB proteins from *C. sinensis* (118) and *A. thaliana* (126). Subgroups within each clade were given
755 a different color; meanwhile, the same color indicates the genes are in the same subgroup. Subgroup
756 short names are included next to each clade to simplify nomenclature. Subgroups that evolved and
757 expanded exclusively in the *C. sinensis* genome are highlighted in red and marked with a red star.

758

759 **Figure 2**. Phylogenetic analysis of the candidate subgroups in six plant species. A neighbor-joining
760 phylogenetic tree was constructed with the R2R3-MYB proteins from *C. sinensis*, *Actinidia*
761 *chinensis*, *Vitis vinifera*, *Theobroma cacao*, *Coffea canephora* and *Arabidopsis* genomes. Subgroup
762 short names are indicated beside each clade.

763

764 **Figure 3**. Analysis of R2 and R3 domains of *C. sinensis* R2R3-MYB TFs. The sequence logos of
765 the R2 (A) and R3 (B) MYB repeats were determined via multiple sequence alignment of the R2R3-
766 MYB proteins. The bit score indicates the information content for each position in the sequence.
767 Highly conserved Trp residues critical for DNA binding in the MYB domain are highlighted in red.

768 **Figure 4**. Phylogenetic relationships and conserved motifs of *C. sinensis* R2R3-MYB TFs. The
769 neighbor-joining tree of 118 R2R3-MYB proteins is shown on the left, and the structures of 20
770 conserved motifs in R2R3-MYB TFs, predicted by MEME Suite, are shown on the right.

771

772 **Figure 5**. Heatmap of the 118 *CsR2R3-MYB* genes transcribed in the tissues of *C. sinensis*. The 118
773 *CsR2R3-MYB* genes clustered into seven expression groups, based on their tissue-specific
774 expression. The gene name is indicated on the left of the heatmap, and the short name of the
775 phylogenetic subgroup is on the right. Transcript abundance is expressed in standardized log2
776 fragments per kilobase of exon per million fragments mapped (FPKM) values. Next to each RNA-
777 seq-based cluster, there is a graph with the mean transcript abundance for the entire cluster in each
778 tissue. AB, apical bud; YL, young leaf; ML, mature leaf; OL, old leaf; S, stem; R, root; Fl, flower;
779 Fr, fruit. Data were obtained from the Tea Plant Information Archive (http://tpia.teaplant.org/).

780

781 **Figure 6**. Expression pattern analysis and correlation analysis of tea-specific or tea-expanded
782 *CsR2R3-MYB*s. (A) The biosynthetic pathway of catechins. *CHS*, *CHI*, *F3H*, *F3'H*, *F3'5'H*, *DFR*,
783 *ANS*, *LAR*, *ANR* and *SCPL1A* represent genes encoding chalcone synthase, chalcone isomerase,
784 flavanone 3-hydroxylase, flavonoid 3'-hydroxylase, flavonoid 3',5'-hydroxylase, dihydroflavonol
785 4-reductase, anthocyanidin synthase, leucoanthocyanidin reductase, anthocyanidin reductase and
786 type 1A serine carboxypeptidase-like acyltransferases, respectively. (B) The contents of six catechin
787 monomers in eight tissues. (C) Heatmap of RNA-seq transcript abundance patterns of the 20
788 *CsR2R3-MYB* genes from the *C. sinensis* genome in eight different tissues. AB, apical bud; YL,
789 young leaf; ML, mature leaf; OL, old leaf; S, stem; R, root; Fl, flower; Fr, fruit. (D) Correlative
790 analysis of *CsR2R3-MYB* genes, structural genes and catechins accumulation patterns in eight
791 representative tissues of *C. sinensis* plants. R>0.5 indicates a positive correlation; R<-0.5 indicates
792 a negative correlation. Data were obtained from the Tea Plant Information Archive
793 (http://tpia.teaplant.org/).

794

Figure 7. Expression profiling validation and correlation analysis. (A) The contents of six catechin monomers in seven tissues as measured with an HPLC system. (B) Heatmap of qRT-PCR transcript abundance patterns in seven different tissues. (C) Correlative analysis of four potential *CsR2R3-MYB* TFs, catechin biosynthesis genes and catechin accumulation patterns in different tissues of tea plants. R>0.5, positive correlation; R<-0.5, negative correlation. AB, apical bud; YL, young leaf; SL, second leaf; ML, mature leaf; OL, old leaf; S, stem; R, root.

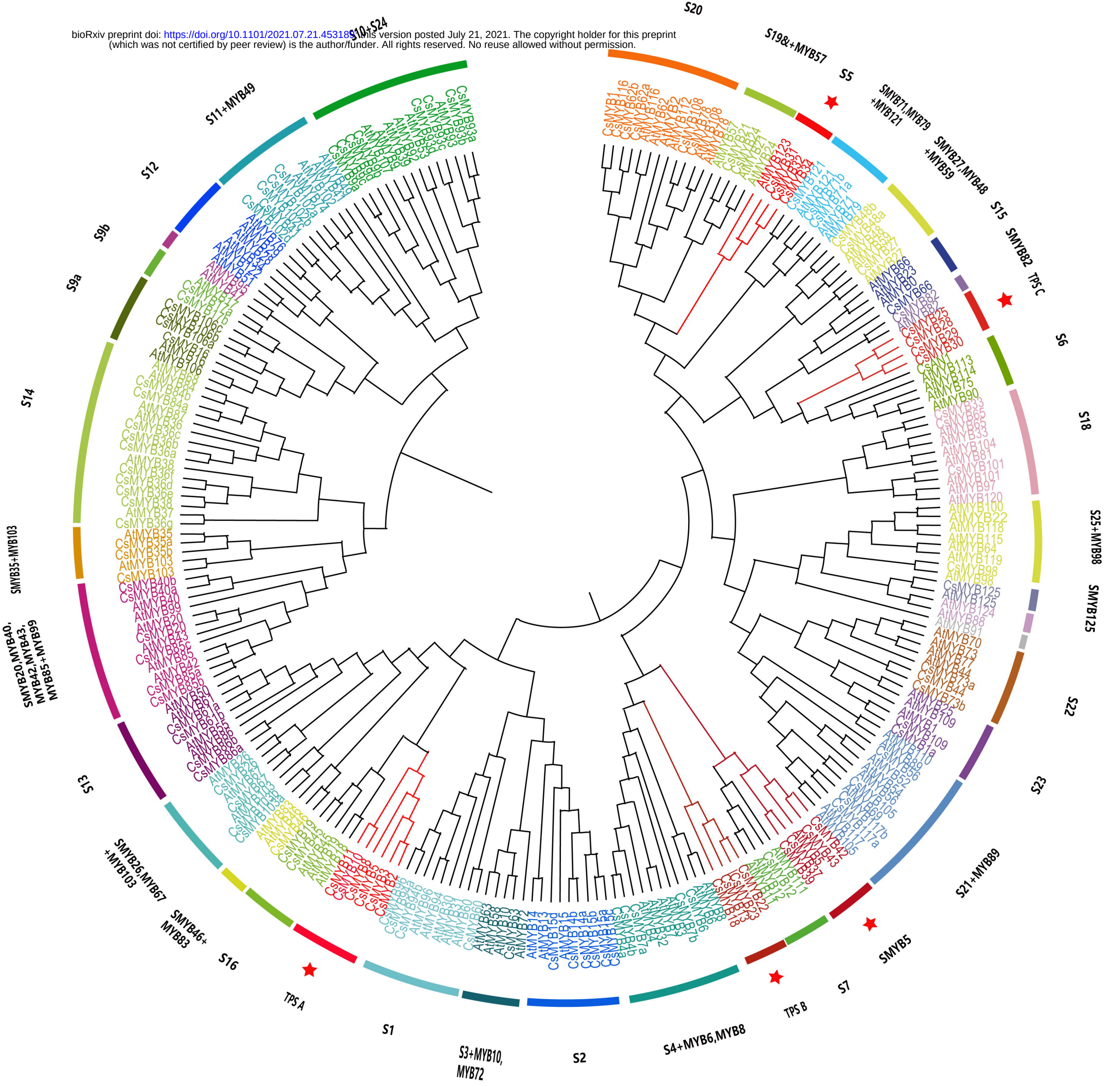

TPS C

TEA004616|CsMYB28
TEA000825|CsMYB25
TEA029017|CsMYB30
TEA001090|CsMYB29
Thecc1EG029121t1
GSVIVT01016765001
GSVIVT01035467001
Thecc1EG037383t1
Cc04_g01360
Thecc1EG015933t1
GSVIVT01006275001

SMYB5

GSVIVT01027182001
Thecc1EG005112t1
TEA014311|CsMYB37
TEA027333|CsMYB39
Thecc1EG015685t1
Cc08_g16530
AT3G13540.1|AtMYB5
GSVIVT01033418001
Thecc1EG025910t1
Thecc1EG024180t1
GSVIVT01025452001
Achn148821
Achn366791
TEA012130|CsMYB42
TEA012145|CsMYB43

S5

AT5G35550.1|AtMYB123
Thecc1EG000535t1
GSVIVT01035462001
Thecc1EG037379t1
TEA004608|CsMYB1
Thecc1EG037559t1
GSVIVT01036633001
GSVIVT01015101001
GSVIVT01015102001
Thecc1EG037555t1
TEA002308|CsMYB32
GSVIVT01015100001
Cc08_g03110
Cc04_g01380
Thecc1EG029121t1
GSVIVT01016767001
TEA031375|CsMYB34
Achn199471

TPS B

Cc11_g08820
Cc11_g08830
GSVIVT01008401001
GSVIVT01008402001
Thecc1EG036404t1
TEA033191|CsMYB18
Thecc1EG012631t1
TEA025886|CsMYB13
Achn294101
Thecc1EG019261t1
GSVIVT01030866001
GSVIVT01011768001
Thecc1EG010839t1
Achn322351
Achn143561
TEA032503|CsMYB23
TEA022874|CsMYB22

TPS A

TEA033589|CsMYB3
TEA027012|CsMYB2
Achn382471
TEA006889|CsMYB5
GSVIVT01000450001
Thecc1EG007868t1
Cc05_g09910
Cc05_g09870
Cc05_g09900
Cc05_g05880
Achn382461
Achn172901
TEA033593|CsMYB8
Cc05_g05740
Thecc1EG007865t1
GSVIVT01000449001
Thecc1EG030020t1
TEA017225|CsMYB10
TEA022451|CsMYB11
Achn111951
Achn030851

0.10

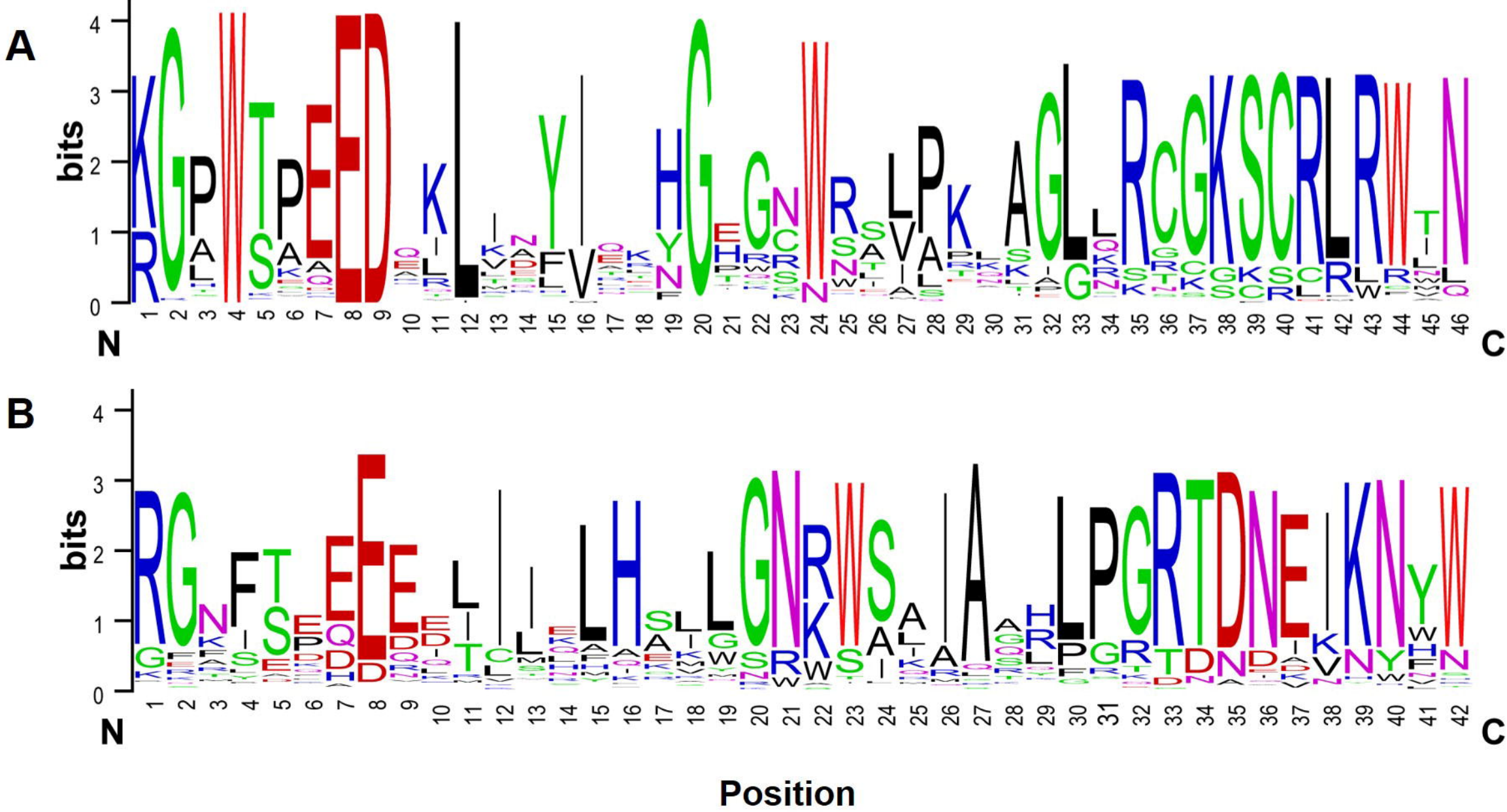
A
bits
N
C
B
bits
N
C
Position

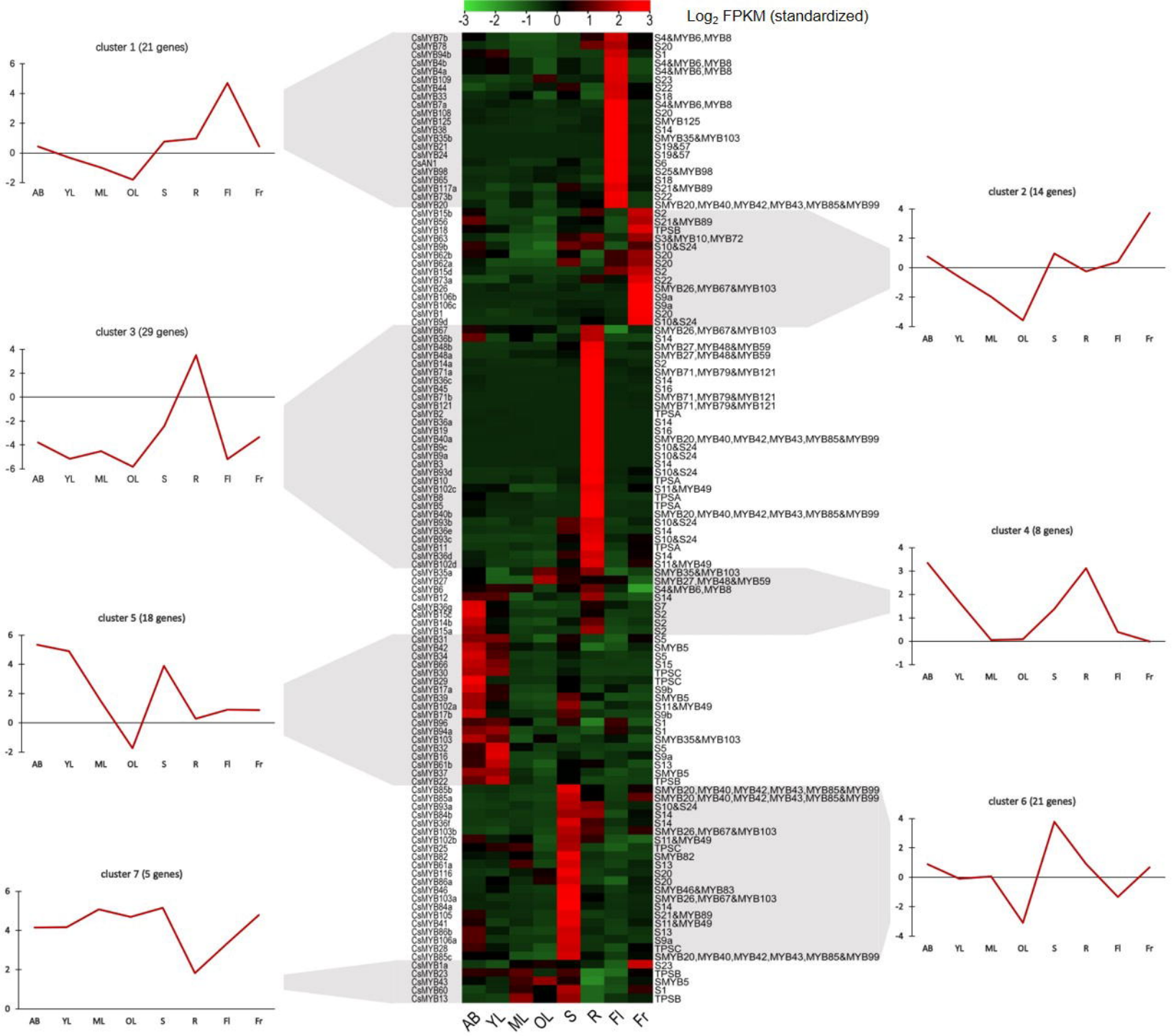
Log2 FPKM (standardized)
-3 -2 -1 0 1 2 3
cluster 1 (21 genes)
cluster 2 (14 genes)
cluster 3 (29 genes)
cluster 4 (8 genes)
cluster 5 (18 genes)
cluster 6 (21 genes)
cluster 7 (5 genes)
AB YL ML OL S R Fl Fr
CsMYB7b S4&MYB6,MYB8
CsMYB78 S20
CsMYB94b S1
CsMYB4b S4&MYB6,MYB8
CsMYB4a S4&MYB6,MYB8
CsMYB109 S23
CsMYB44 S22
CsMYB33 S18
CsMYB7a S4&MYB6,MYB8
CsMYB108 S20
CsMYB125 SMYB125
CsMYB38 S14
CsMYB35b SMYB35&MYB103
CsMYB21 S19&57
CsMYB24 S19&57
CsAN1 S6
CsMYB98 S25&MYB98
CsMYB65 S18
CsMYB117a S21&MYB89
CsMYB73b S22
CsMYB20 SMYB20,MYB40,MYB42,MYB43,MYB85&MYB99
CsMYB15b S2
CsMYB56 S21&MYB89
CsMYB18 TPSB
CsMYB63 S3&MYB10,MYB72
CsMYB9b S10&S24
CsMYB62b S20
CsMYB62a S20
CsMYB15d S2
CsMYB73a S22
CsMYB26 SMYB26,MYB67&MYB103
CsMYB106b S9a
CsMYB106c S9a
CsMYB1 S20
CsMYB9d S10&S24
CsMYB67 SMYB26,MYB67&MYB103
CsMYB36b S14
CsMYB48b SMYB27,MYB48&MYB59
CsMYB48a SMYB27,MYB48&MYB59
CsMYB14a S2
CsMYB71a SMYB71,MYB79&MYB121
CsMYB36c S14
CsMYB45 S16
CsMYB71b SMYB71,MYB79&MYB121
CsMYB121 SMYB71,MYB79&MYB121
CsMYB2 TPSA
CsMYB36a S14
CsMYB19 S16
CsMYB40a SMYB20,MYB40,MYB42,MYB43,MYB85&MYB99
CsMYB9c S10&S24
CsMYB9a S10&S24
CsMYB3 S14
CsMYB93d S10&S24
CsMYB10 TPSA
CsMYB102c S11&MYB49
CsMYB8 TPSA
CsMYB5 TPSA
CsMYB40b SMYB20,MYB40,MYB42,MYB43,MYB85&MYB99
CsMYB93b S10&S24
CsMYB36e S14
CsMYB93c S10&S24
CsMYB11 TPSA
CsMYB36d S14
CsMYB102d S11&MYB49
CsMYB35a SMYB35&MYB103
CsMYB27 SMYB27,MYB48&MYB59
CsMYB6 S4&MYB6,MYB8
CsMYB12 S14
CsMYB36g S7
CsMYB15c S2
CsMYB14b S2
CsMYB15a S2
CsMYB31 S5
CsMYB42 SMYB5
CsMYB34 S5
CsMYB66 S15
CsMYB30 TPSC
CsMYB29 TPSC
CsMYB17a S9b
CsMYB39 SMYB5
CsMYB102a S11&MYB49
CsMYB17b S9b
CsMYB96 S1
CsMYB94a S1
CsMYB103 SMYB35&MYB103
CsMYB32 S5
CsMYB16 S9a
CsMYB61b S13
CsMYB37 SMYB5
CsMYB22 TPSB
CsMYB85b SMYB20,MYB40,MYB42,MYB43,MYB85&MYB99
CsMYB85a SMYB20,MYB40,MYB42,MYB43,MYB85&MYB99
CsMYB93a S10&S24
CsMYB84b S14
CsMYB36f S14
CsMYB103b SMYB26,MYB67&MYB103
CsMYB102b S11&MYB49
CsMYB25 TPSC
CsMYB82 SMYB82
CsMYB61a S13
CsMYB116 S20
CsMYB86a S20
CsMYB46 SMYB46&MYB83
CsMYB103a SMYB26,MYB67&MYB103
CsMYB84a S14
CsMYB105 S21&MYB89
CsMYB41 S11&MYB49
CsMYB86b S13
CsMYB106a S9a
CsMYB28 TPSC
CsMYB85c SMYB20,MYB40,MYB42,MYB43,MYB85&MYB99
CsMYB1a S23
CsMYB23 TPSB
CsMYB43 SMYB5
CsMYB60 S1
CsMYB13 TPSB

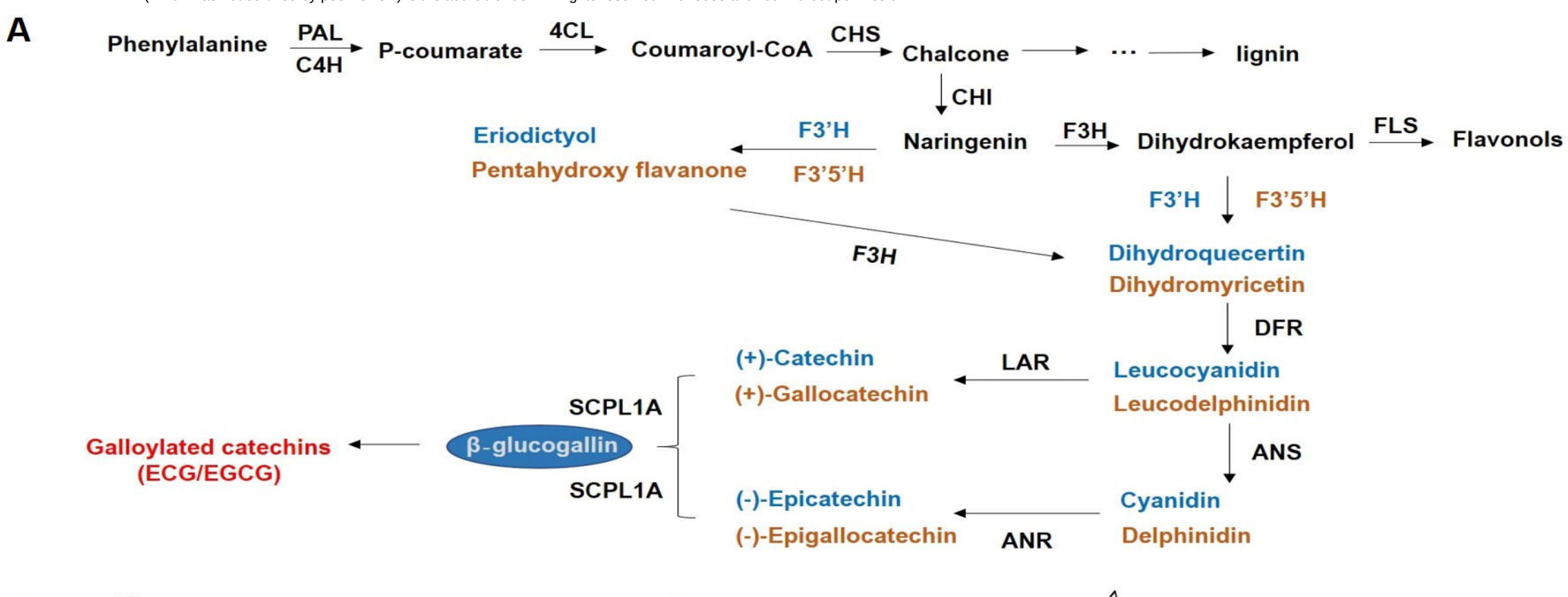
A
Phenylalanine
PAL
C4H
P-coumarate
4CL
Coumaroyl-CoA
CHS
Chalcone
···
lignin
CHI
Eriodictyol
Pentahydroxy flavanone
F3'H
F3'5'H
Naringenin
F3H
Dihydrokaempferol
FLS
Flavonols
F3'H
F3'5'H
F3H
Dihydroquecertin
Dihydromyricetin
DFR
(+)-Catechin
(+)-Gallocatechin
LAR
Leucocyanidin
Leucodelphinidin
SCPL1A
β-glucogallin
Galloylated catechins
(ECG/EGCG)
SCPL1A
ANS
(-)-Epicatechin
(-)-Epigallocatechin
ANR
Cyanidin
Delphinidin

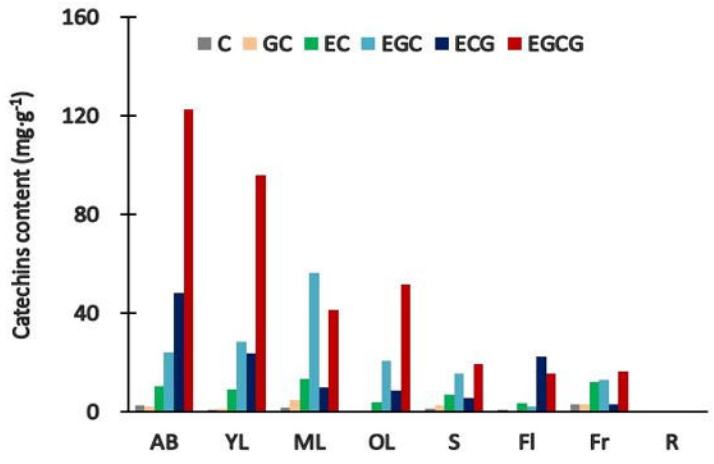
B
C
EC
EGC
ECG
EGCG
Catechins content (mg·g-1)
160
120
80
40
0
AB
YL
ML
OL
S
Fl
Fr
R

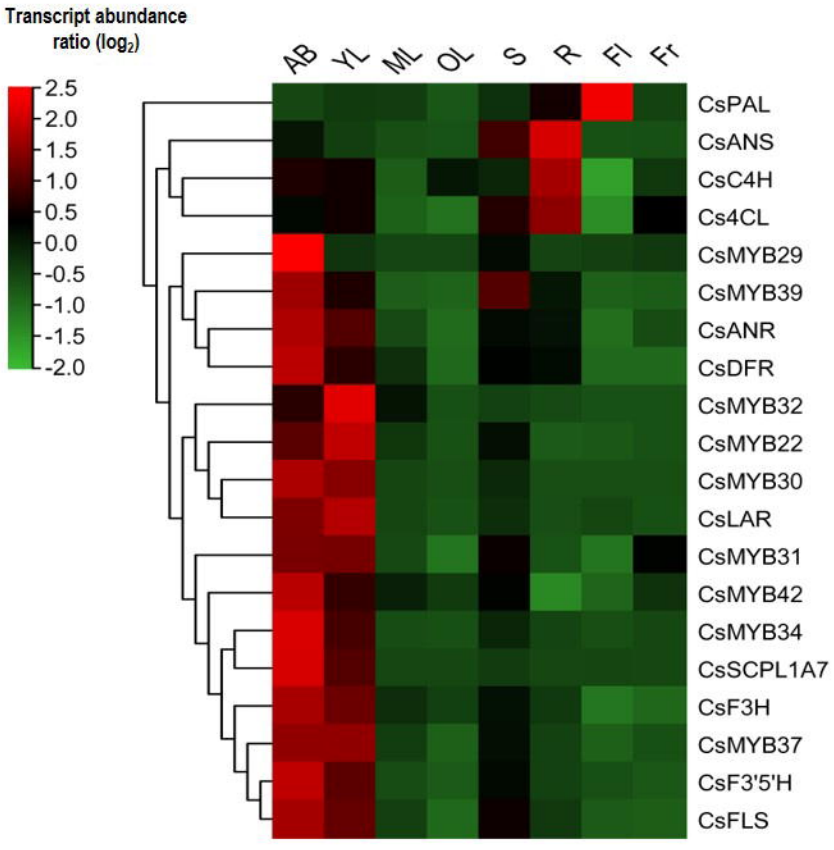
C
Transcript abundance
ratio (log2)
2.5
2.0
1.5
1.0
0.5
0.0
-0.5
-1.0
-1.5
-2.0
AB
YL
ML
OL
S
R
Fl
Fr
CsPAL
CsANS
CsC4H
Cs4CL
CsMYB29
CsMYB39
CsANR
CsDFR
CsMYB32
CsMYB22
CsMYB30
CsLAR
CsMYB31
CsMYB42
CsMYB34
CsSCPL1A7
CsF3H
CsMYB37
CsF3'5'H
CsFLS

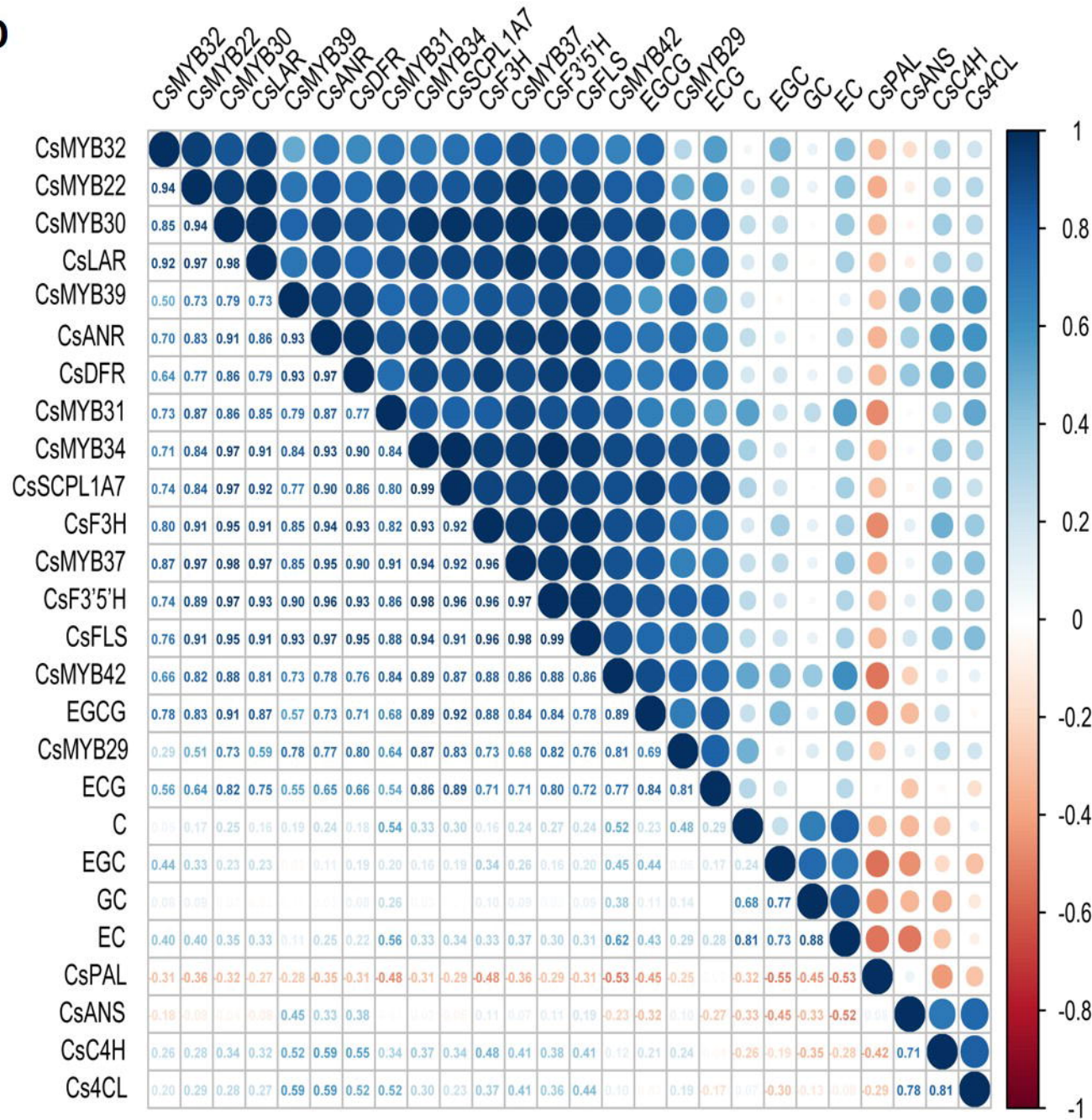
D
CsMYB32
CsMYB22
CsMYB30
CsLAR
CsMYB39
CsANR
CsDFR
CsMYB31
CsMYB34
CsSCPL1A7
CsF3H
CsMYB37
CsF3'5'H
CsFLS
CsMYB42
EGCG
CsMYB29
ECG
C
EGC
GC
EC
CsPAL
CsANS
CsC4H
Cs4CL
1
0.8
0.6
0.4
0.2
0
-0.2
-0.4
-0.6
-0.8
-1

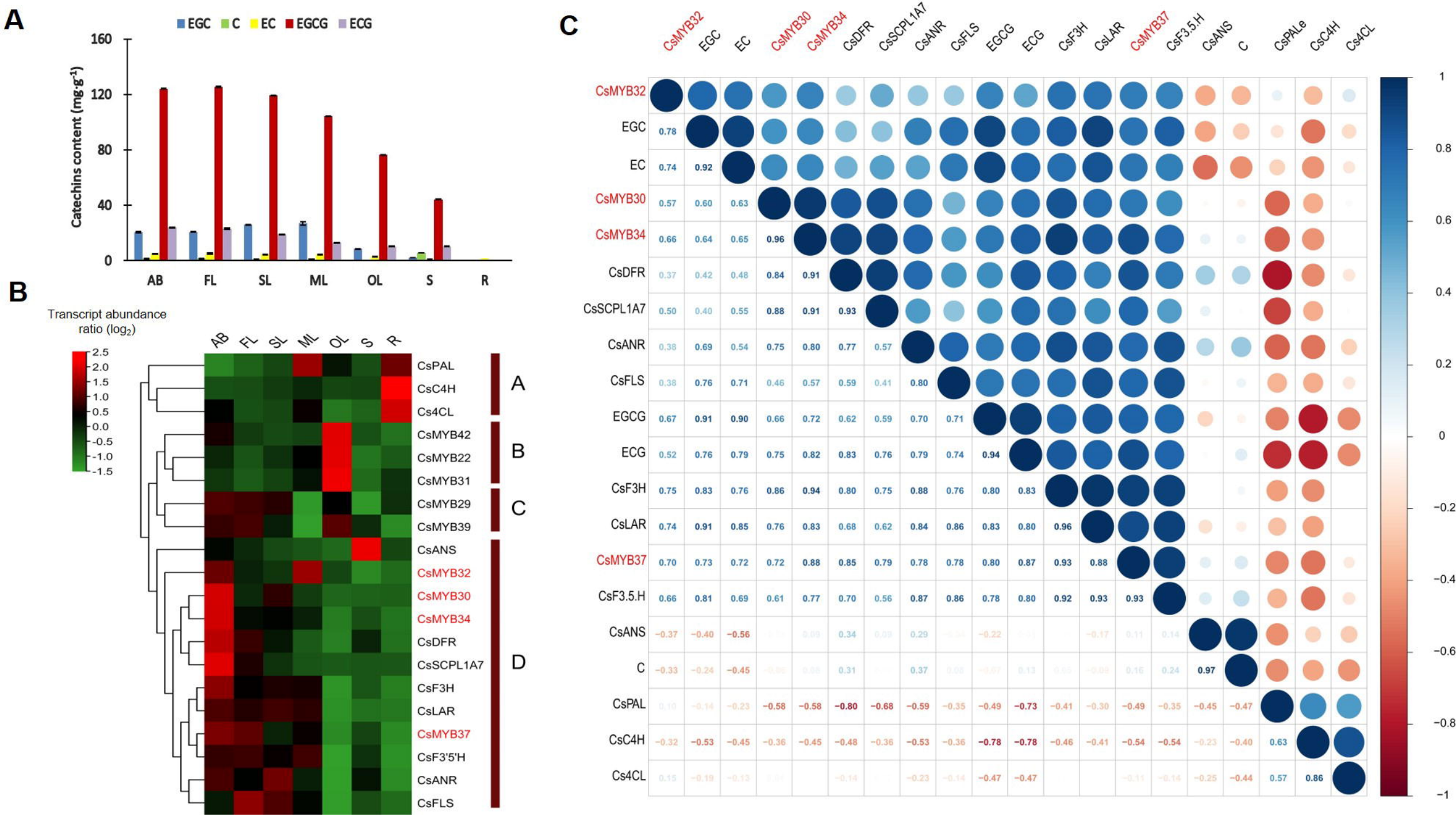
A
EGC
C
EC
EGCG
ECG
Catechins content (mg·g⁻¹)
160
120
80
40
0
AB
FL
SL
ML
OL
S
R
B
Transcript abundance ratio (log2)
2.5
2.0
1.5
1.0
0.5
0.0
-0.5
-1.0
-1.5
AB
FL
SL
ML
OL
S
R
CsPAL
CsC4H
Cs4CL
CsMYB42
CsMYB22
CsMYB31
CsMYB29
CsMYB39
CsANS
CsMYB32
CsMYB30
CsMYB34
CsDFR
CsSCPL1A7
CsF3H
CsLAR
CsMYB37
CsF3'5'H
CsANR
CsFLS
A
B
C
D
C
CsMYB32
EGC
EC
CsMYB30
CsMYB34
CsDFR
CsSCPL1A7
CsANR
CsFLS
EGCG
ECG
CsF3H
CsLAR
CsMYB37
CsF3'5.H
CsANS
C
CsPALe
CsC4H
Cs4CL
1
0.8
0.6
0.4
0.2
0
−0.2
−0.4
−0.6
−0.8
−1